Check for updates

Received: 23 April 2020 | Revised: 23 September 2020 | Accepted: 9 October 2020

DOI: 10.1002/gea.21831

RESEARCH ARTICLE

Geoarchaeology An International Journal WILEY

Revisiting Alice Boer: Site formation processes and dating issues of a supposedly pre-Clovis site in Southeastern Brazil

Astolfo G. de Mello Araujo[1] | James K. Feathers[2] | Gelvam A. Hartmann[3,4] | Francisco S. B. Ladeira[3] | Éverton V. Valezio[3] | Diego L. Nascimento[3] | Olivia Ricci[5] | Victor J. de Oliveira Marum[6] | Ricardo I. Ferreira da Trindade[7]

[1]Museum of Archaeology and Ethnology, University of São Paulo, Butantã, São Paulo, Brazil

[2]Department of Anthropology, University of Washington, Seattle, Washington, USA

[3]Department of Geography, Geoscience Institute, State University of Campinas, Campinas, São Paulo, Brazil

[4]Department of Geology and Natural Resources, Institute of Geosciences, University of Campinas, Campinas, São Paulo, Brazil

[5]Museum of Archaeology and Ethnology, University of São Paulo, Butantã, São Paulo, Brazil

[6]Department of Mining and Petroleum Geology, University of São Paulo, São Paulo, São Paulo, Brazil

[7]Department of Geophysics, Institute of Astronomy, Geophysics, and Atmospheric Sciences, University of São Paulo, São Paulo, Brazil

Correspondence
Astolfo G. de Mello Araujo, Museum of Archaeology and Ethnology, University of São Paulo, Av. Prof. Almeida Prado, 1466 Cidade Universitária, Butantã, CEP 05508-070 São Paulo, Brazil.
Email: astwolfo@usp.br

Funding information
Fundação de Amparo à Pesquisa do Estado de São Paulo, Grant/Award Numbers: 2009/54.720-9, 2013/13.794-5, 2016/23.584-6; Conselho Nacional de Desenvolvimento Científico e Tecnológico, Grant/Award Numbers: 300339/2008-9, 302024/2019-0, 307951/2018-9, 308629/2015-9

Scientific editing by Vance Holliday

Abstract

The Alice Boer site, located in Southeastern Brazil, was considered to be one of the oldest sites in the Americas, and a strong candidate for being a pre-Clovis site. Ages obtained by researchers during the 1970s and 1980s put the site inside a chronological range between 2 and 14 ka, eventually reaching as old as 30 ka or even 130 ka. Between 2010 and 2012, our research team revisited the site to improve the knowledge of Paleoindian occupation in Southeastern Brazil. Here, we present new data of stratigraphy and chronology (luminescence and radiocarbon dating), pedological and magnetic analysis performed at some of the sites. Results show that the site's oldest occupation took place ca. 8 ka, which provides new insight into human occupation in South America. In addition, we show some issues with radiocarbon contamination due to soil humin fraction mobility.

KEYWORDS

Alice Boer, geoarchaeology, humin dating, pre-Clovis, site formation processes

1 | INTRODUCTION

The ages and dispersal routes related to the peopling of the Americas are still subjects of open debate (e.g., Araujo, 2015; Boëda et al., 2014; Braje et al., 2020; Dillehay et al., 2008; Fiedel, 2017; O'Brien et al., 2014; Parenti et al., 2018; Stanford & Bradley, 2012; Vialou et al., 2017), comprising a stimulating field of research where specific sites and models come and go. One example, the Alice Boer site, excavated between 1961 and 1986 by Maria Beltrão from the National Museum of Rio de Janeiro, was considered to be one of the major candidates for being a pre-Clovis site. The site showed a very early radiocarbon age of 14,200 ± 1150 BP obtained by the Smithsonian Institute and published in Portuguese (sample SI-1208; Beltrão, 1974). On the basis of this age, the author stated that by means of "stratigraphic interpolations," the site could be at least 20,000-years old (Beltrão, 1974, p. 246). Citations of the site in the international literature followed in the 1970s, both in French (Laming-Emperaire, 1975, 1976) and English (Gruhn, 1977;

 © 2020 Wiley Periodicals LLC

MacNeish, 1976, 1978), and the site entered the hall of "early sites" of South America (Bryan & Beltrão, 1978). In the 1980s, more ages were published, including luminescence of sediments and burnt chert (Beltrão et al., 1982, 1983; Poupeau, Cunha, et al., 1984; Poupeau, Souza, et al., 1984) and the site continued to be cited as a potential candidate to be the oldest site from South America (e.g., Beattie & Bryan, 1984; Bednarik, 1989; Gruhn, 1988; Hurt, 1986).

Toward the end of the 1980s, critiques of the ages and the nature of artifacts from Alice Boer started to accumulate (e.g., Bate, 1990; Calderón & Politis, 1989; Fagan, 1987; Lynch, 1990; Schmitz, 1990). In the 1990s, Gruhn and Bryan (1991) made a rebuttal of Lynch's (1990) observations about Alice Boer, which caused a heated debate (Lynch, 1991) but Lynch maintained his position through the years (e.g., Lynch, 1998, p. 90). The site continued to appear in synthesis papers (e.g., Dillehay et al., 1992; Whitley & Dorn, 1993). More critiques followed (e.g., Prous, 1995; Prous & Fogaça, 1999), without any rebuttal by Beltrão, whose interests shifted toward rock art sites with purported Pleistocene ages elsewhere (e.g., Beltrão & Andrade Lima, 1986).

Scattered mentions to Alice Boer continued to be found in the literature (Dillehay, 1999; Roosevelt, 1998). Scheinsohn (2003, p. 345) mentions the "rejection" of Alice Boer as an early site, but without citing references. On the contrary, in Dillehay et al. (2008, p. 31) the site appears as a dot on the map showing "early archaeological sites in South America," and in Steeves (2015, p. 56) it appears in a table as being earlier than 12,000 ^{14}C BP, but in both papers references about the site are absent. Careless attributions one way or another are obviously deleterious for a scientific debate because there are no strong data to either support or reject Alice Boer as a late Pleistocene site. Here, we present new data to clarify some issues regarding the site's chronology, stratigraphy, and formation processes. As a collateral contribution, our data show some trends regarding the dating of soil organic matter (SOM) that runs counter to the common wisdom that the humin fraction is an extremely stable SOM component, practically immovable and, therefore, reliable as a chronological marker.

2 | GEOLOGICAL AND GEOMORPHOLOGICAL CONTEXT

Alice Boer is located in the Rio Claro region, São Paulo State, Southeastern Brazil (Figure 1). Both the geology and geomorphology of the area are linked to the sediments of the Paraná Basin, an intracratonic sedimentary basin formed between the Upper Ordovician and the Upper Cretaceous (Milani & Zalan, 1999). At Rio Claro, the geologic deposits related to the final stages of sediment infilling are the Corumbataí Formation argilites (Upper Permian/Lower Triassic), the Botucatu Formation sandstones (Upper Jurassic/Lower Cretaceous), and the Serra Geral Formation basalts (Lower Cretaceous; Pereira et al., 2012). During the Tertiary, fluvial sediments of the Itaqueri Formation (Ladeira, 2002) and Rio Claro Formation (Zaine, 1994) were deposited on the top of the sequence (Figure 2). The Itaqueri Fm. shows deposits of alluvial fans with soil formation episodes (Ladeira & Santos, 2006), whereas the Rio Claro Fm. is composed of unconsolidated sandy deposits formed by a meandering fluvial system (Fúlfaro & Suguio, 1968; Melo, 1995; Zaine,1994).

From the geomorphological point of view, the area is located in the limit between two large morphostructural units, the Western Plateau ("Planalto Occidental") and the Peripheric Depression (Depressão Periférica; see Pinheiro & Queiroz Neto, 2014; Ross & Moroz, 1997). At least three planation surfaces were recognized in the area (Penteado, 1968): The summit surface, around 1000 m a.s.l.; the Urucaia Surface, between 720 and 690 m a.s.l., and the Rio Claro Surface, around 600 m a.s.l. (Figure 2). Related to a more recent chronological framework, Penteado (1968) recognized three terrace levels: t3, 40 to 50 m above the base level (a.b.l.); t2, around 15 to 20 m a.b.l., and t1, 4 to 6 m a.b.l.

Alice Boer site is located on a terrace of the Cabeça river (t1), 100 m before the confluence with the Passa Cinco river (Figure 1). The terrace is sandy and its top is currently 4 m above the river level (Figure 3). Preliminary observations, coupled with previously published data (Meis & Beltrão, 1982) strongly suggested that at the time of human occupation the river was higher and closer to the site than at present.

3 | ALICE BOER: A META-ANALYSIS

We first analyze the published data about Alice Boer to better understand the site setting and the problems related to the stratigraphy and also the positioning of both ages and artifacts within the stratigraphy. From the available papers, it was possible to estimate the relative positioning of the excavation areas, but no sketch plan was formally published. In our first visits to the site, we could observe the presence of depressions in the ground that was probably due to erosion of the walls and partial infilling of the units that were left open for more than 30 years. However, based on the published data, positive identification was impossible. The original maps and stratigraphic profiles published along the years were also not very informative, because either of print quality and size of the figures, or the absence of graphic scales. For example, in Beltrão (1974, p. 219) and Bryan & Beltrão (1978, p. 304), the stratigraphic profile of the site appears with an indication of a "1:25 scale," leaving the reader with no clue about its actual size. The same happens in Beltrão et al. (1983, p. 29) where a "typical stratigraphic column" of the site is presented without any scale, together with the information on the legend that "the total thickness of the outcrop is of the order 4 to 5 m (sic)." A more detailed stratigraphic profile, including a graphic scale, was published in Meis and Beltrão (1982, p. 409), but the authors do not mention which unit it represents. Later publications (e.g., Beltrão, 2008, p. 28, 34) continued to present stratigraphic profiles without scale.

After some research into the "gray literature," we found a detailed unpublished report written by Poupeau, Cunha, et al. (1984), and an unpublished MA thesis by Perez (1991). Due to the sketches, profiles, and photographs contained in these works, we were able to

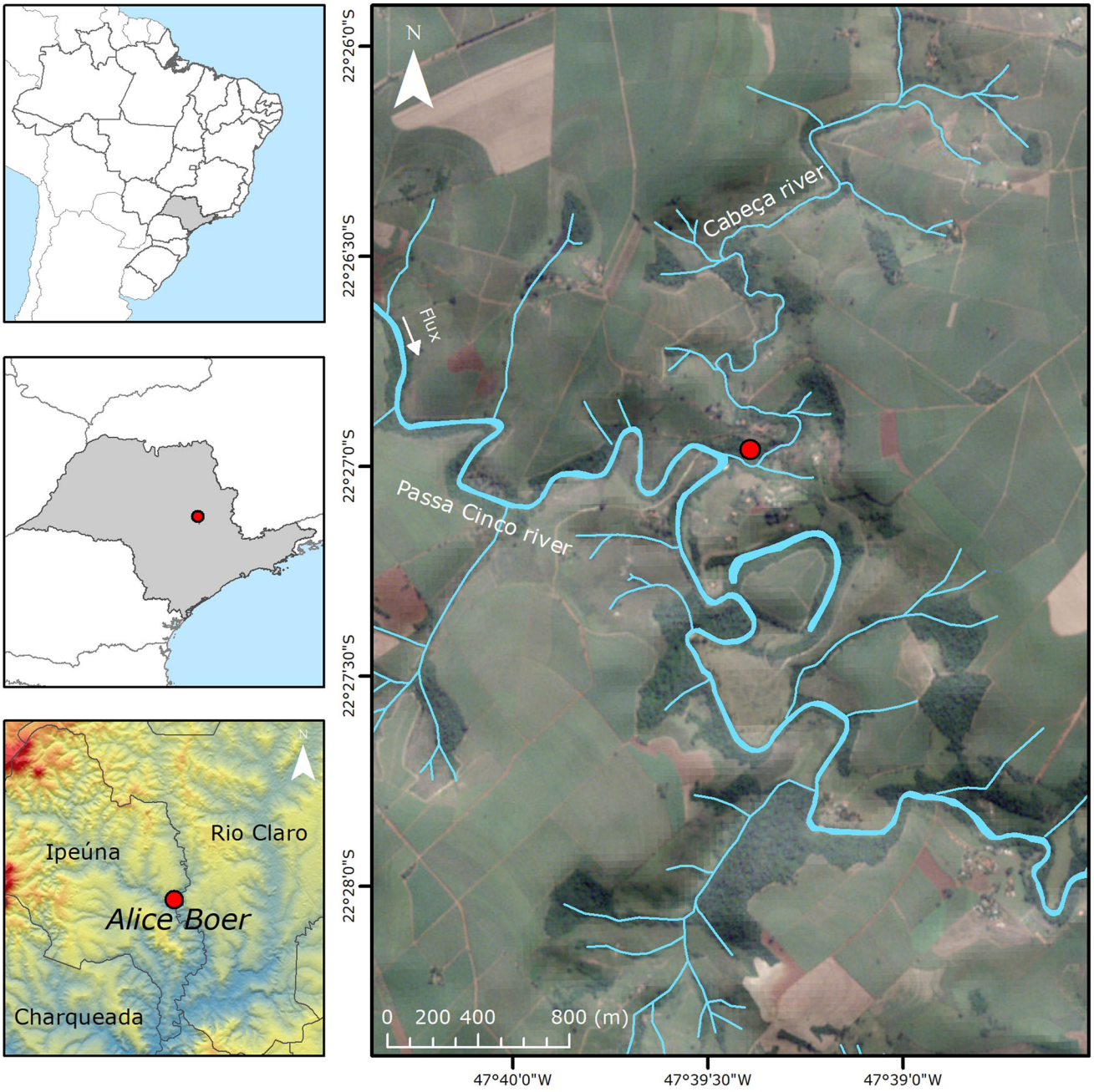

FIGURE 1 Location of Alice Boer site in Southeastern Brazil [Color figure can be viewed at wileyonlinelibrary.com]

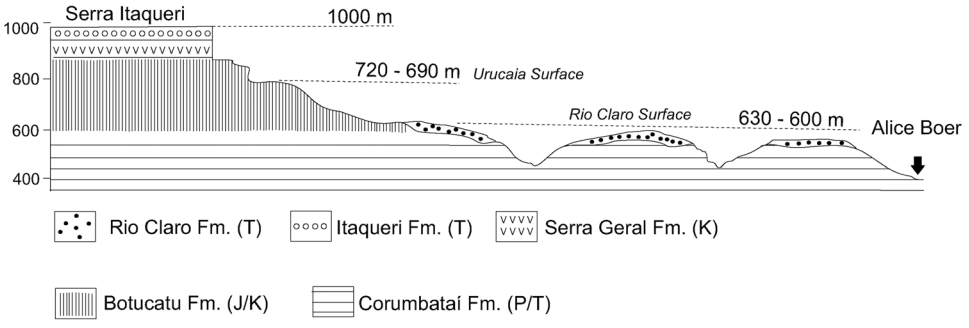

FIGURE 2 Geological and geomorphological sketch of Rio Claro region

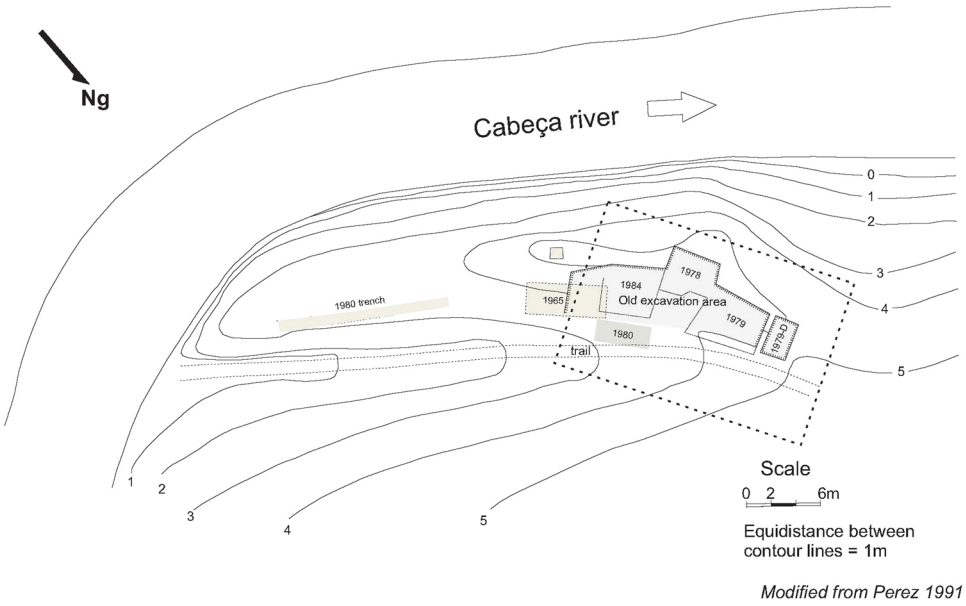

FIGURE 3 Topographic map showing the location of the previous excavations and the relation between the site and the Cabeça river. Modified from Perez (1991) [Color figure can be viewed at wileyonlinelibrary.com]

understand the exact positioning of the excavation units (Figure 4). Some of the depressions observed in the field were indeed collapsed excavation units, but some of the excavated units were apparently backfilled, leaving no trace on the surface.

The first excavations were carried out in 1965 (although, as we will see, there is mention of a "1961/64" excavation) by M. Beltrão, covering an extension of 6 m, reaching a depth of 4 m on the right side of a small path that descends from the farm's headquarters to the river (Figures 3 and 4, marked as "1965"). This path was situated in a small depression, which has, as a border on both sides, the ravine walls that rise about 4 m high from the lower part (Beltrão, 2000, p. 11). This excavation was probably backfilled, and no trace of its position can be detected nowadays.

Another fieldwork season occurred in 1978/79, concentrating the excavations near the area worked in 1965, in the sediment belt located to the right of the access road to the Cabeça River. Three excavation areas (or "trenches") were opened, two on the west side and one on the east side of the trail: The first, on a surface of 3 m in the N–S direction, 4 m in the E–W direction and 3.20 m in depth. The second was 3-m wide, with the same orientation as the previous one and reached 3.09-m deep (*op cit*: 11–12). Both can be seen in Figure 4, marked as "1978" and "1979." These two excavation units were left open and they can be seen nowadays. The third trench reached 2-m deep and an area of 4 × 3 m excavated on the east side of the trail, over the ravine, with the intention of checking the stratigraphic and cultural continuity. This trench has proved to be totally sterile from the archaeological point of view, and consisted of alternating layers of large, small, or medium-sized rolled pebbles and sand. Its position was never marked on any sketch map of the site, and was probably backfilled.

In February 1980, there was another intervention, where "sectors SIII and SIV" were excavated. Twenty-eight dosimeters were placed for luminescence dating, but only two were subsequently found in situ (*op cit* 2000:13). It is marked in Figure 4 as "1980." This excavation was probably backfilled and no trace of it can be seen on surface.

In July 1980, the team opened 10 test-pits in the areas near the site, a new trench to locate and explore Layer V (riverbed), in addition to topographic surveying for geological purposes. According to the authors, the test-pits did not provide relevant data for the archaeological interpretation. The trench for the exploration of Layer V, located along the path on the right bank, advanced southward toward the Cabeça river. The depth reached was 1.50 m and in it was found some archaeological material. Its position is shown in Figure 3, marked as the "1980 trench."

In January 1984, another intervention was done with the objective of (a) relocating the excavated area in 1961/64; (b) select a new area to be excavated; (c) proceed to the observation of the sedimentology to verify the rhythm of sedimentation; (d) determine the thickness of all layers, according to archaeological stratigraphy; (e) collect sand samples, for dating through thermoluminescence. The newly selected area was delimited in 3.60 m of length by 4 m of width. It was located on the terrace, in its residual portion, to the right (west) of the trail that leads to the Cabeça river, about 40 m from the latter, directly in front of the trench opened in July 1980, and south of the squares excavated in 1978. The area was open according to the system of steps, following the natural inclination of the layers (*op cit*:13–14). Its position is marked in Figure 4 as "1984," and it was probably backfilled.

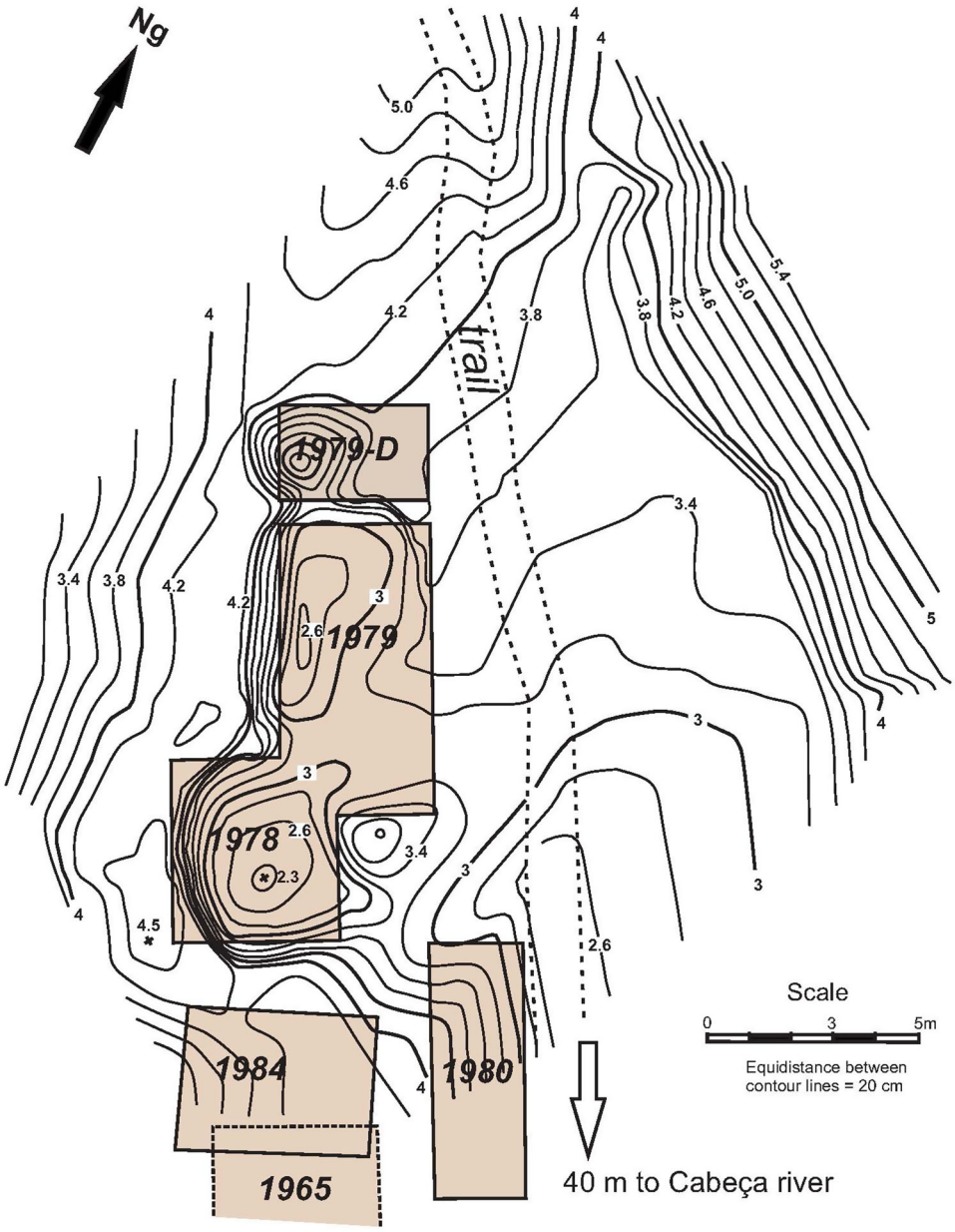

FIGURE 4 Alice Boer site. Detailed topographic map with the location of the former excavation areas, after Poupeau, Cunha, et al.,1984 [Color figure can be viewed at wileyonlinelibrary.com]

3.1 | The stratigraphy of the site according to previous publications

The stratigraphy of the site was represented in different ways over time. The older publications (Beltrão, 1974; Bryan & Beltrão, 1978) use a nomenclature in Roman numerals. The most recent publications, derived from collaborations with Earth Science professionals (Meis & Beltrão, 1982), use a nomenclature based on Arabic numerals, subdividing some of the "archaeological" layers. Such correlation can be observed in Figure 5, modified from Poupeau, Cunha, et al. (1984). Again, Figure 5 does not show a scale, making difficult the assessment of the actual site depth.

According to the publications, stratigraphy can be described as follows, from top to bottom:

Layer I: Sterile from the archaeological point of view, with a few inches of depth, covered by current vegetation.

Layer II: Sterile from the archaeological point of view, about 1.40-m thick "would correspond to the colluvium (…) transported by surface sliding, from the highest points of the slope. This layer, which shows no signs of stratification, would correspond to a dry phase [sic] with concentrated rains, which would have started some 3,500 years ago. From the base of this layer, the environmental conditions are approximately the same as the present" (Beltrão, 1974, 2000).

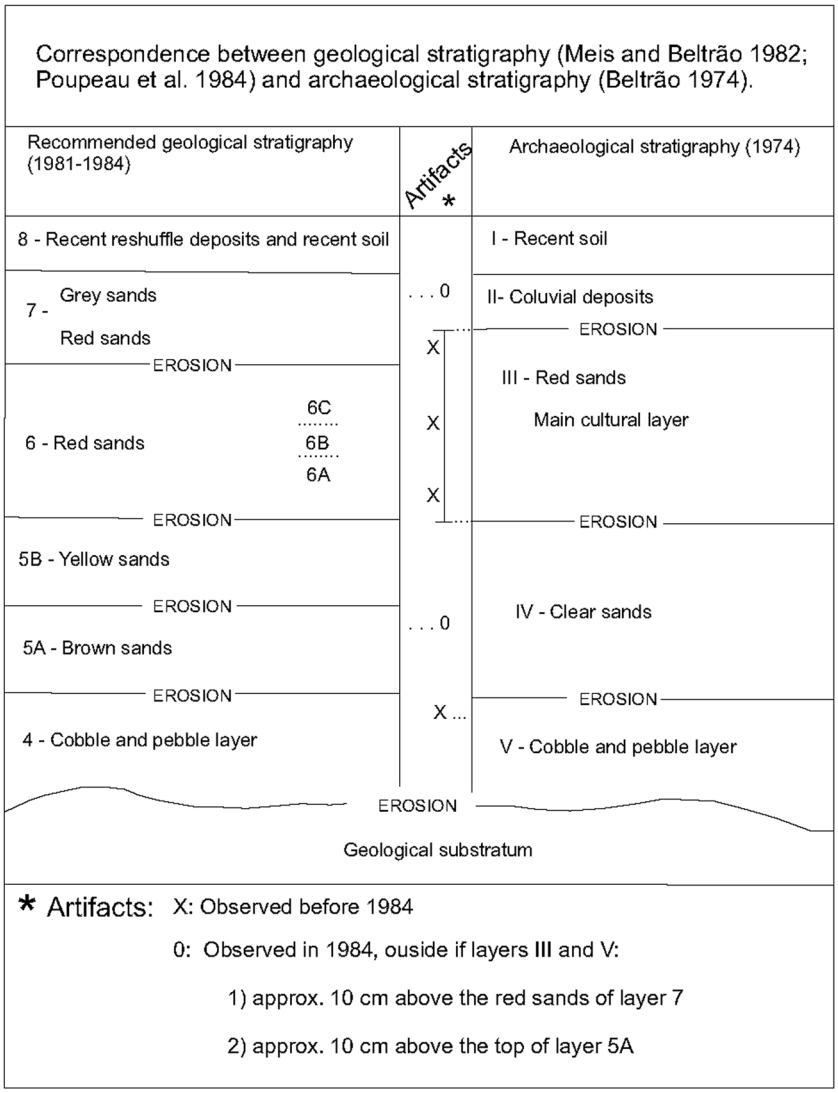

FIGURE 5 Correlation between the "geological" and "archaeological" nomenclature of the Alice Boer Site (modified from Poupeau, Cunha, et al., 1984)

Layer III: Rich in archaeological materials, composed of silt and clay, about 2-m thick, "and correspond to a hot and humid phase, with thick forest cover. This climatic phase allowed the decomposition of more friable rocks, such as siltites and argillites" (Beltrão, 1974, 2000).

Another description of Layer III:

> *Alluvial sands composing Bed III, contained unclearly differentiated layers disturbed by ants, so excavations within that bed were carried out by artificial 10-cm levels. All 19 levels yielded artifacts or good flakes.*
>
> (Bryan & Beltrão, 1978)

In Beltrão (2000) Layer IIIa is defined as "sand-compact red clay," and IIIb (lower) as "noncompacted red-yellow sand, with an erosive discontinuity between these two layers. These same layers are called "6" and "7" in Meis and Beltrão (1982).

Layer 7 is the IIIa, upper, comprising thin and coarse sandy deposits, quartzous, and relatively poorly selected, with visible mottling by iron oxides in their basal portion. It shows the predominance of cross strata of planar type. Flint artifacts were also found within this unit (Meis and Beltrão, 1982, p. 407).

> *These younger stratified sands, which constitute the younger cycle, cut all the previously described sedimentary bodies and show the occurrence of artifacts flaked of chert. These young, yellowish and mottled sands are considered to be of Holocene age.*
>
> (Meis & Beltrão, 1981)

Layer 6 is the lower IIIb, composed of a series of reddish materials, fine and coarse sand with possible enrichment in quartz granules and silts, showing a very unclear stratification and iron oxide concentration, being "a unit rich in lithic artifacts" (Meis & Beltrão, 1982).

This layer showed "a succession of stratified and bioturbated fine to coarse sands, locally enriched with silts and mottled reddish colors. During the geological expedition a large amount of artifacts carved in chert were found inside the cross-stratified sands" (Meis & Beltrão, 1981).

Between Layers III and IV, there is another erosive discordance.

Layer IV: Sterile from the archaeological point of view, this layer is a sand deposit similar to those that exist in the current margin of the Cabeça river. "This deposit was left in that position by the river, when it wandered, leaving a meander and deepening its bed, 130,000 years ago or more. The sand deposit is not stratified (…) which would indicate sedimentation under a torrential regime. This light, washed sand, sits atop layers and pebbles from the Layer V" (Meis & Beltrão, 1981).

> *The second unit is heterogeneous from the lithological point of view, with its base constituted by rounded quartz pebbles along with fresh basalt and diabase boulders.*
>
> (Meis & Beltrão, 1981)

Layer V: Presenting archaeological material, "corresponds to the old river bed, with more than 130,000 years A.P. [sic] and a semi-arid climate phase, more than the current one" (Meis & Beltrão, 1981).

It is worth noting that in the 1974 publication, the author puts the age of abandonment of the meander around 30,000 BP, not 130,000 BP.

> *The first unit, of rudaceous nature, is characterized by the relative abundance of weathered basalt and diabase pebbles and boulders. (op. cit.)*

3.2 | Chronology according to previous publications

Regarding the chronology obtained for the site, the data compiled appear as follows:

Layer III was dated by 14C and thermoluminescence (TL). The layer was excavated in artificial levels of 10 cm due to its supposed homogeneity, which, however, is not suggested by later publications. The radiocarbon ages were published in Beltrão (1974) and those of TL on heated chert were published in Beltrão et al. (1982); Table 1 shows the relationships between the ages obtained and their respective levels. The authors did not present sample numbers or the exact location of the samples. We can only assume, based on the chronology of publications, that all radiocarbon samples were collected in the "1965" excavation area, whereas the TL samples were collected in the "1980" area (see Figures 3 and 4).

There is a clear discrepancy in the TL ages obtained for Level 4 of Layer III, which were too recent in relation to ^{14}C, and in Level 8, where the opposite occurs, with much older TL ages on heated chert. However, it is important to note that these results can be obtained if the lithics were not heated high enough.

Poupeau, Cunha, et al. (1984) and Poupeau, Souza, et al. (1984) collected another 20 samples for luminescence dating, showing the sketches of each profile with the locations of the samples and a site sketch map showing all the excavation units. The location of the samples aimed to answer several questions related to both the formation of the site and the age of the artifacts found, but we did not find any formal publication with the results. In any case, it was from this unpublished report that we were able to understand the layout of the excavation units (Figure 4).

3.3 | The archaeological remains

The only class of archaeological materials reported by previous publications is lithics. A PhD dissertation on the topic was done in France by L. Cunha, when 4000 pieces from the earlier excavation seasons (1964 to 1968) were analyzed (Cunha, 1994; see also Perez, 1991, p. 144); later, an M.A thesis regarding aspects of raw material treatment (especially heat-treatment) was done in Brazil by Perez (1991). There is no mention of the finding of combustion features, faunal, or macrobotanical remains. Charcoal fragments were rare, hence the reliance on TL for constructing the site chronology.

The lithic industry was characterized as showing bifacial points and unifacially retouched scrappers (Beltrão, 1974; Perez, 1991). The bifacial points were later analyzed both in their morphological (Okumura & Araujo, 2016) and technological (Moreno de Sousa, 2019) aspects. A more detailed account of the archaeological aspects of the site is shown in Araujo et al. (2020).

TABLE 1 Alice Boer site, "Layer III," renamed "Layers 6 and 7"

Level	Age BP (method)
1	2200 ± 280 (TL) 2370 ± 220 (TL) 2000 ± 200 (TL)
2	N/A
3	6050 ± 100 (^{14}C)
4	2870 ± 450 (TL) 3400 ± 200 (TL)
5	6135 ± 160 (^{14}C)
6	N/A
7	6350 ± 1220 (TL)
8	6085 ± 160 (^{14}C) 10,970 ± 1020 (TL) 10,950 ± 1020 (TL)
9	N/A
10	14,200 ± 1150 (^{14}C)

Note: Relationship between artificial levels and ages obtained by radiocarbon (^{14}C) and thermoluminescence (TL). It is important to note that the levels represent 10-cm spits inside the layer and are not directly related to the site surface.

4 | MATERIALS AND METHODS: THE 2010–2012 INTERVENTIONS

4.1 | General aspects

The main objective of our interventions at Alice Boer was to collect samples to confirm the age of the site, given the conflicting nature of the previously obtained data. Currently, the area of the site is covered by a gallery forest. The vegetation had two roles in the preservation of the site: On the one hand, the tree roots protected the profiles left open by the previous excavations; on the other hand, these same roots would greatly hinder the work of rectifying the profiles.

Among the three profiles still visible in the field, only one was suitable to be worked without the need of cutting the thick roots, which could compromise the stability of the sandy sediment. With the help of Poupeau's report (Poupeau, Cunha, et al., 1984), we could diagnose that the most suitable place for the beginning of the interventions was the west profile of the "1979" excavation, according to the plan presented in Figure 4.

Once the place of the intervention was chosen, we established points for topographical anchoring, installed topography equipment, and began cleaning and rectifying the profile by careful scraping with trowels. As soon as the work began, flakes of varying sizes started to appear in the profile. Each of these pieces was plotted by means of a total station, which allowed us to reconstitute the geometry of the archaeological layer. The dimensions were taken in millimeters, using the level of the river at the time of the work as the arbitrary datum. At the end of the work, 362 pieces were plotted (Figure 6).

We also opened a trench on the floor of the unit excavated by Beltrão in 1979 to verify if we could reach the basal gravel, originally denominated "Layer V" (Beltrão, 1974). In this gravel, Beltrão claimed to have found artifacts (Beltrão, 2000) and our purpose was to collect sediment samples for a set of analyzes, in addition to material for dating. Some additional excavation units were opened. One of them was placed on the extant fluvial beach to observe if charcoal particles produced by hearths lit by fishermen were preserved in the stratigraphy.

4.2 | Sediment and dating sampling

Sediment samples for general purposes, such as granulometric characterization, were collected in a column in the west profile of the 1979 excavation. The same samples were quartered and used for both microartifact and magnetic analysis (see Sections 4.4 and 4.5).

We also collected samples for luminescence dating, following two protocols: (a) The most traditional pounding of metallic or PVC (polyvinyl chloride) pipes inside the profile and (b) the collection of sandy sediments found between clasts of the basal conglomerate, where the insertion of the pipes would be impossible. This was done by covering the excavation with tarps, using red lights for visualization, and scraping and shoveling the sediment inside the pipe. This last procedure was tested before in another site (see Araujo & Feathers, 2008) and provided good results. All optically stimulated luminescence (OSL) samples were processed at the Luminescence Dating Laboratory,

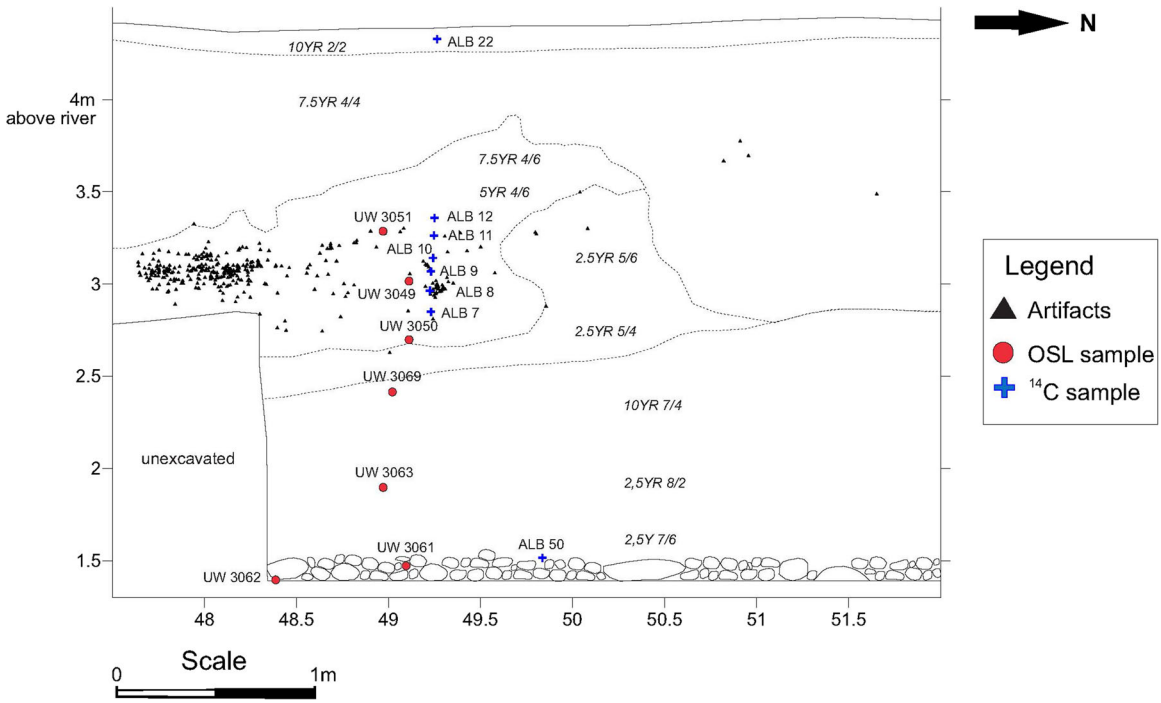

FIGURE 6 Alice Boer site. West profile of the 1979 excavation unit showing the placement of archaeological materials and dating samples [Color figure can be viewed at wileyonlinelibrary.com]

University of Washington. The sample material was removed from the collection container, leaving aside any portions that may have been exposed to light. From the unexposed portions, about a quarter was set aside as a voucher (material that can be used at a later date, if necessary). Remaining unexposed material was separated into size fractions by sieving. The fractions greater than 90 μm were treated with HCl and H_2O_2, rinsed three times with water and dried. They were then dry-sieved to retrieve the 180- to 212-μm fraction. This fraction was etched for 40 min in flouridric acid and then rinsed with water, HCl, and water again. After drying, it was passed through a 180-μm screen to remove any degraded feldspar. To isolate quartz, the material caught in the screen was density separated using a lithium metatungstate solution of 2.67 specific gravity.

Equivalent dose (D_e), which is a measure of the total absorbed dose through time, was determined on single grains of quartz using the single-aliquot regenerative dose (SAR) protocol (Murray & Wintle, 2000, Wintle & Murray, 2006).

The dose rate, or the estimate of the amount of environmental radioactivity received by the sample in a given interval of time, was measured by alpha counting in conjunction with atomic emission (flame photometry) for ^{40}K. The pairs technique was used to separate the U and Th decay series. Radioactivity was also measured, as a check, by beta counting, using a Risø low-level beta Geiger–Muller multicounter system. The average of four subsamples was converted to dose rate following Bøtter-Jensen and Mejdahl (1988) and compared with the beta dose rate calculated from the alpha counting and flame photometer results. Cosmic radiation was determined after Prescott and Hutton (1988). Radioactivity concentrations were translated into dose rates following Guérin et al. (2011).

Radiocarbon samples comprised either soil or small charcoal fragments. Samples were sent to Beta Analytic Inc., following the standard protocols. Sediment samples were treated by acid/alkali/acid procedure. Only the humin (alkali-insoluble) fraction was analyzed (not total SOM).

4.3 | Soil description and micromorphology sampling

The west profile of the 1979 excavation was macromorphologically described from top to bottom (until the conglomerate contact), where the pedogenetic horizons were identified and characterized by differences in color, texture, and pedogenetic structure differences (Santos et al., 2005) and classified following Embrapa—Empresa Brasileira de Pesquisa Agropecuária (2006) and FAO—Food and Agriculture Organization (2014). The top of the terrace profile is ca. 4 m above the current river.

Seven undisturbed soil samples were collected for thin sections (30 × 40mm) in the transitions of the identified horizons. The thin sections were processed at the Lamination Laboratory of the São Paulo State University (UNESP) at Rio Claro, and the pedofeatures and microstructures were observed by means of a Leica DM750 P optical microscope. The thin sections and the micromorphological features were described according to Bullock et al. (1985) and Stoops et al. (2018), and the size ranges according to Udden (1914) and Wentworth (1922).

The chemical soil analysis quantified the pH conditions ($CaCl_2$, H_2O and SMP); Ca, K, and Mg exchangeable (ion-exchange resin method); Al exchangeable (extracted with KCl); potential acidity (H + Al); sum of bases (*S*); Soil cation exchange capacity; organic matter (OM); and base saturation (*V*). The analyses were performed at Unithal Technology Laboratory, Campinas, State of São Paulo.

4.4 | Microartifact analysis

Thirty-eight sediment samples (or 19 paired samples) taken from the column at the west profile, 1979 excavation, were processed in the Sedimentology Laboratory of the Institute of Geosciences, University of São Paulo. Samples with 50 g collected at each 10-cm level were mixed with deflocculant sodium pyrophosphate in a mechanical shaker for 10 min, then washed in a 4-phi sieve (0.063 mm) for disposal of the silt and clay fraction, oven-dried at 35° for at least 6 h, and shaken on 0 to 4-phi sieves (2–0.063 mm). Each fraction was properly weighed and stored.

Samples were also processed using the Wagner (rotative) shaker. In this case, the samples were weighed (using 50 g of each level), mixed with deflocculant sodium pyrophosphate and agitated in the Wagner shaker for 12 h, washed in 4-phi sieve (0.063 mm) to discardsilt and clay, dried in beakers placed in a 300°C sand bath for about 3 h or sufficient for total drying of the sample and shaken on 0- to 4-phi sieves (2–0.063 mm) and each fraction was properly weighed and stored. We used both methods to verify if different shakers imparted differences in the microartifact frequencies, but the results were inconclusive (Ricci, 2018).

Microartifact analysis was based on the protocol of Vance (1989), which consists of the following steps: quarter the sediment sample, using a maximum of 200 g, an inspection of the 1-phi fraction (between 0.5 and 0.25 mm), spread the 1-phi fraction on the Petri dish and counting 2000 grains. We made a modification on the protocol, analyzing not only the fraction between 0.5 and 0.25 mm, but also the fraction between 1 and 0.5 mm.

4.5 | Magnetic analysis

Magnetic measurements were carried out on 19 specimens from the west profile, 1979 excavation (18.9- to 185.2-cm depth). Magnetic experiments were performed at the Laboratório de Paleomagnetismo of Universidade de São Paulo (USPMmag). Magnetic analysis of low-field magnetic susceptibility (χ or MS), natural remanent magnetization (NRM), anhysteretic remanent magnetization (ARM), and isothermal remanent magnetization (IRM) were used here to determine the different magnetic contributions throughout the profile of the site. Enhancement of magnetic contribution can be associated

with variations in soil development or firing (Evans & Heller, 2003). The low-field MS (χ) measurements of each specimen were taken using an MFK1-A Kappabridge (AGICO, Ltd.) with a 200-A/m field oscillating at both 976 Hz (F1) and 15,616 Hz (F2) excitation frequencies for calculating the frequency-dependent MS χfd% (χfd% = [(χF1 − χF3)/χF1] × 100). Increasing of χfd% coupled with an increment in MS indicates an increase in the percentage of superparamagnetic (SP) grains within the total assemblage of magnetic grains. SP contribution is often observed in burned or well-developed soils (e.g., Dalan & Banerjee, 1998).

NRM, ARM, and IRM measurements were performed using a vertical 755-1.65 UC SQUID magnetometer (2G Enterprises) housed in a magnetically shielded room with an ambient field <500 nT. The ARM acquisition curves were acquired with a bias field of 0.05 mT in 22 steps up to 100 mT. This technique is used to obtain magnetic mineralogy by determining some parameters, such as median destructive field ($B_{1/2}$) and the dispersion parameter (e.g., Kruiver et al., 2001; Maxbauer et al., 2016a, 2016b). Both parameters provide the oxidation state of magnetic minerals and then it will be able to establish which alteration process those magnetic minerals were submitted to (Egli, 2004). The IRM data were obtained using a pulse magnetizer with applied DC fields of +1000 mT (corresponding to the saturation of IRM, SIRM) and a backfield of −300 mT. The *S*-ratio of each sample was determined using a ratio of IRM magnetizations, that is, *S*-ratio = [|IRM-300 mT|/|SIRM|]. *S*-ratio indicates the relative contribution of high-coercivity minerals (e.g., hematite, goethite) to low-coercivity minerals (e.g., magnetite, maghemite; see Evans & Heller, 2003; Liu et al., 2012). From the IRM data, we also computed the high-coercivity isothermal remanent magnetization (HIRM), that is, HIRM = [|SIRM − IRM-300 mT|/2]. HIRM is frequently used to isolate signals due to high coercivity minerals (e.g., hematite, goethite) to magnetite or maghemite. Both MS and remanent magnetizations were all normalized by mass.

5 | RESULTS

5.1 | Spatial positioning of archaeological materials

The tridimensional plotting of 362 recovered pieces allowed us to evaluate the main aspects of the archaeological layer still present in the profile. Figure 6 shows the overlapping of the pieces (black triangles) on the profile. Almost all pieces are debitage, with the exception of a unifacially retouched flake (see details in Araujo et al., 2020) and were found mostly on the left (south) portion of the profile (Figure 6). However, this distribution does not necessarily reflect the reality since the southern portion of the profile was the most excavated, considering that the profile was originally abutted by erosion, and we had to rectify it. Therefore, more relevant than the number of pieces in the profile, the main information obtained was their vertical dispersion. Figure 7 shows the vertical distribution of the pieces in 10-cm intervals. The simple inspection of Figure 7 allows us to infer two characteristics of the archaeological deposit: (1) Most of the pieces (89.7%) are placed in a vertical interval of only 30 cm, between depths of 110–140 cm (2.90 and 3.10 m above the river); (2) the distribution of the pieces is strongly unimodal, suggesting that originally there would be a single archaeological layer, placed between 120- and 130-cm deep (around 3.0 m above the current level of the river. The pieces above and below may have been displaced by bioturbation (see discussion below, and also Araujo, 1995, 2013).

Results for microartifact analysis are shown in Table 2. Only two categories of microscopic finds were detected: (1) microflakes resulting from flaking activities and/or resharpening and (2) charcoal particles. The graphic representation of the microartifact and charcoal particle frequencies for 0.25- and 0.5-mm fractions combined are shown in Figure 8. Our data confirm the absence of botanical and faunal remains in the site, both microscopically and macroscopically, as well as the rarity of large charcoal fragments.

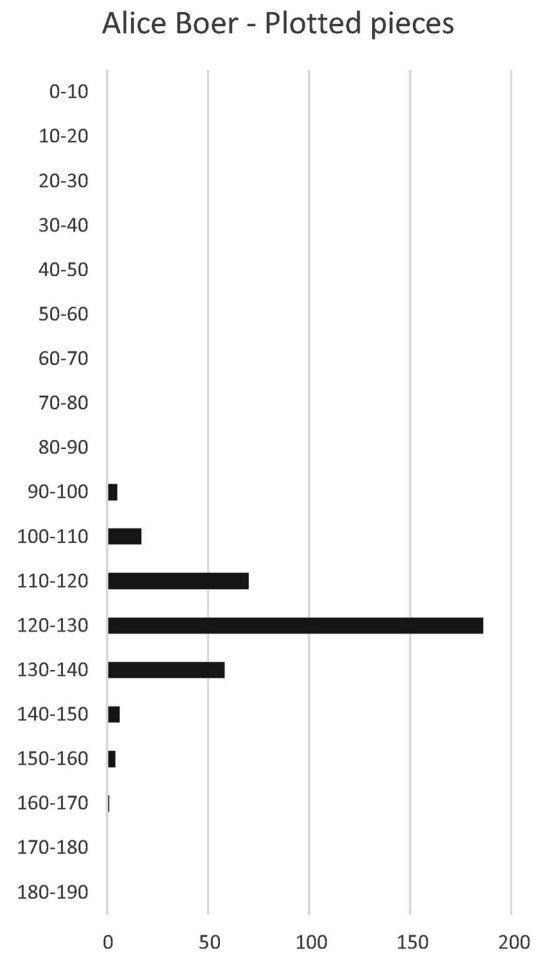

FIGURE 7 Alice Boer site, west profile of the 1979 excavation. Frequency of pieces found by vertical intervals of 10 cm

TABLE 2 Alice Boer site, west profile of the 1979 excavation

	0.5-mm fraction—Wagner		0.25-mm fraction—Wagner		0.5-mm fraction—mechanic		0.25-mm fraction—mechanic		Total	
Level (cm)	Microart	Charcoal	Microart	Charcoal	Microart	Charcoal	Microart	Charcoal	Microart	Charcoal
0–10	0	0	0	0	0	0	0	0	0	0
10–20	0	3	0	3	0	0	0	0	0	6
20–30	0	0	0	0	0	0	0	3	0	3
30–40	0	3	0	3	0	0	0	2	0	8
40–50	0	0	0	0	0	0	0	0	0	0
50–60	0	0	0	1	0	1	1	1	1	3
60–70	1	1	0	1	0	0	0	0	1	2
70–80	0	1	1	2	0	0	0	0	1	3
80–90	1	0	1	0	0	0	0	1	2	1
90–100	0	5	0	0	0	0	0	3	0	8
100–110	0	1	0	0	0	0	0	2	0	3
110–120	0	2	0	0	0	1	0	2	0	5
120–130	0	0	0	1	1	3	1	1	2	5
130–140	0	0	1	0	1	2	2	2	4	4
140–150	0	1	1	0	0	0	1	6	2	7
150–160	0	1	0	0	2	4	1	2	3	7
160–170	0	3	0	3	0	3	0	1	0	10
170–180	0	0	0	0	2	0	0	0	2	0
180–190	0	0	0	0	0	0	0	0	0	0

Note: Frequency of microartifacts and charcoal particles by depth, using different methods, 2000-grain count.

5.2 | Soil horizons and stratigraphy

From the macroscopic point of view, the site stratigraphy is composed of a very homogeneous column of sandy soil, without observable structures (Figure 9). The major differences observed across the profile are related to its color and some pedogenic features. Nine soil horizons were determined, and the results of morphology and chemical analysis enabled us to separate the profile into two different soils. One of the soil profiles consists of horizons A, C1, C2, C3, C4 and C5; the other comprises horizons 2C1, 2C2, and 2C3. A morphological discontinuity was observed between the 2C1 and C5 horizons (Figure 9). Only the A horizon presented blocky and crumb structures, visible with the unaided eye, and attributed to an accumulation of OM and root activity. The soils show brownish, reddish, and yellowish colors (Table 3) with a poor degree of development, in spite of an increase in clay content in the lower horizons, producing sandy to clayey textures at C3 and C4 horizons. Some mottles and redoximorphic features were observed associated with roots and krotovinas (2 cm on average) filled with materials from the upper horizons, mainly in the 2C1 horizon. The presence of these features identifies a horizon representing an old surface, indicating a paleosurface at the level of 160-/178-cm depth.

The micromorphological aspects of topsoil (A, C1, and C2 horizons) show an open porphyric distribution; the coarse fabric components (skeleton grains) were composed of allochthonous material mainly of poorly sorted and rounded quartz grains, feldspar and opaque minerals, without dissolution features. The b-fabric in topsoil is mainly darker with irregular impregnate nodules, crumb microstructure associated with OM accumulation and fine roots (fresh and decomposed) (Figure 10a,b). In the A, C1, C2, and C3 horizons, there are common occurrences of plant tissues, such as root fragments (1.5 mm), besides coalescence fecal pellets (Figure 10c), (0.3 mm). The porosity of the upper horizons is predominantly related to biological origin.

In the lower horizons, pedogenic structures were almost absent (Figure 10d) and the pedofeatures consist of poorly oriented clay coatings and an undifferentiated or dotted b-fabric with quitonic to gefuric (c/f) distribution, indicating a low degree of soil development. In these horizons, OM decreases in quantity, with the predominance of the coarse mineral fraction. However, the occurrence of fecal pellets and micropedofabrics (voids, channels, or aggregates) produced by the faunal activities are common. One example of this is the circular packet aggregates with subcircular or ellipsoidal structure of 1 mm on average (Figure 10e), composed of packet fine-grained

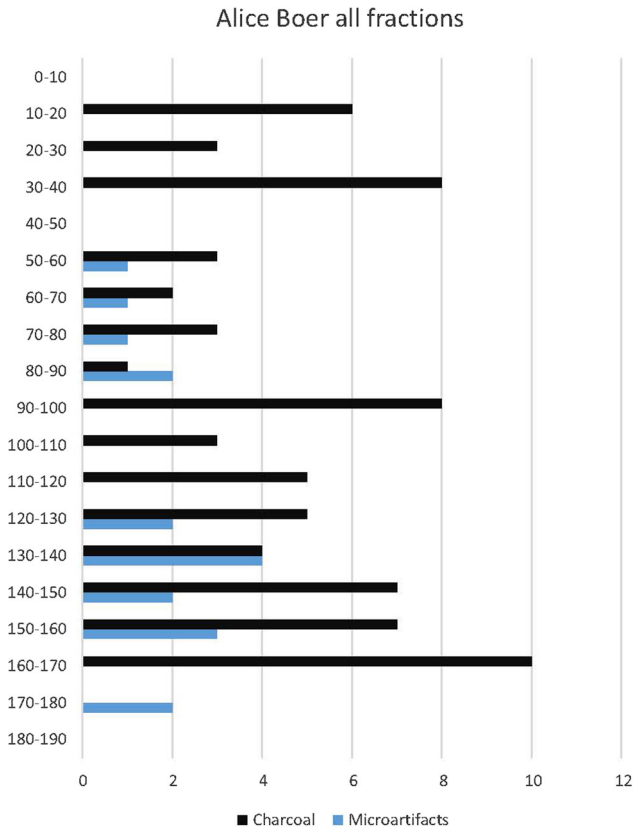

FIGURE 8 Alice Boer site, west profile of the 1979 excavation. Frequency of microartifacts and charcoal particles, 0.25- and 0.5-mm fractions combined, by the depth [Color figure can be viewed at wileyonlinelibrary.com]

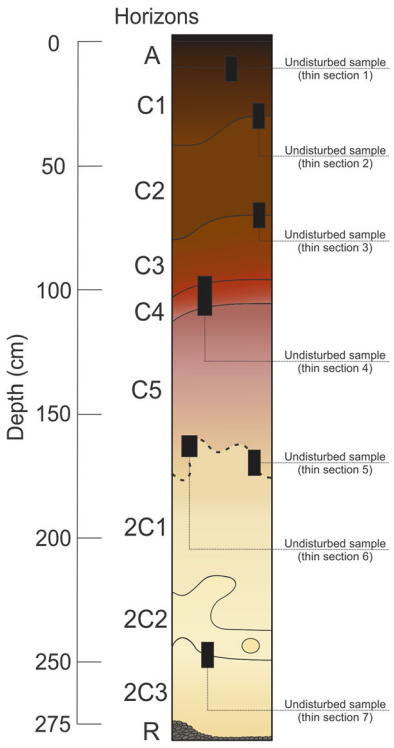

FIGURE 9 Alice Boer site. Soil column and micromorphology samples taken at the west profile of the 1979 excavation [Color figure can be viewed at wileyonlinelibrary.com]

quartz, clay, and OM. These structures present smooth external boundaries, occurring as linings at channel walls or filling channels and voids and are the product of burrowing or excretions by geophage invertebrates (Humphreys, 1993; Kooistra & Pulleman, 2010). The presence of meniscal structures (2 mm) associated with invertebrate feeding behavior is also common (Figure 10f).

The decrease of pH values between C1 and C4 (minimum values in C4) could be correlated to aluminum activity (Table 4). The soil base saturation (*V*) and the potential acidity result from a high degree of weathering and poor pedogenetic development, forming dystrophic horizons inside the overbank quartzose riverine deposits in the upper profile. However, the base saturation is high in the basal profile, with a eutrophic character, supporting the interpretation of two distinct soils within the profile.

Charcoal fragments with an average of 2 mm (Figure 11a,b) occur across the soil horizons associated with the groundmass. These features show the vascular and anatomic structures preserved, with a specific porosity pattern. Another important feature is the presence of knapped lithic artifacts composed of quartz integrating the groundmass coarse fraction (Figure 11c,d). Its identification is given by its geometric or angular shape in comparison to most other components of the groundmass. These shapes include specific delineation and sharp boundaries with scars, which are related to the mechanical behavior of the raw material (Angelucci, 2010; Macphail & Goldberg, 2010). Table 5 shows the micromorphological description of the soils.

According to the macro and micromorphological characteristics, the main pedogenetic features observed along all horizons are the accumulation of OM (topsoil), and biological activity associated with root and invertebrate activity (macromixing, fragmentation, and aggregate formation). The results obtained indicate that biological mixing can be responsible for the divergences in chronology and also for the vertical positioning of the pieces (see Figures 6 and 7).

Lastly, it is important to note that the excavation of the unit close to the river, where several modern hearths made by fishermen can be observed, produced no macroscopic charcoal fragments. This suggests that the water flow is responsible for the removal of charcoal particles.

5.3 | Magnetic results

Magnetic results from the west 1979 excavation profile are shown in Figure 12. The mass-normalized MS presents an increase with depth, varying from ~3.3×10^{-7} m^3/kg (185.2-cm depth) to 1.45×10^{-6} m^3/kg (136.2-cm depth). Around ~18.9- and ~99.2-cm depth, the MS remains constant in their values; from ~99.2- to ~116.8-cm depth, MS presents a slight increase and after decreases from this depth up to ~185.2 cm. The χfd% varies between ~10% and 17% in the entire profile: From ~18.9- and ~99.2-cm depth, the χfd% presents similar values between ~10% and ~12% and after it increases up to ~17%. This behavior suggests an increase in superparamagnetic (SP) grains after ~99.2-cm

TABLE 3 Macromorphological properties of terrace profile

Depth (cm)	Horizon	Color	Structure	Texture	Transition
0–10	A	10YR2/2 Very dark brown	Blocks	Sandy/clay	Abrupt/clear
10–30/42	C1	7.5YR4/4 Brown	Massive	Sandy	Clear/wavy
42–70/80	C2	7YR4/6 Strong brown	Massive	Sandy	Clear/wavy
80–96/110	C3	5YR4/6 Yellowish red	Massive	Sandy/clay	Abrupt/clear
96–110	C4	2.5YR5/6 Red	Massive	Sandy/clay	Abrupt/clear
110–160/178	C5	2.5YR5/4 Reddish-brown	Massive	Sandy	Gradual/wavy
160/178–215/236	2C1	2.5Y7/6 Very pale brown	Massive	Sandy	Gradual/wavy
215/236–241/250	2C2	2.5Y7/2 Pale yellow	Massive	Sandy	Gradual
241/250–275	2C3	2.5Y7/6 Yellow	Massive	Sandy	Abrupt

depth. The *S*-ratio presents values varying between ~0.85 (176.4 cm) and 0.98 (19.2 cm); from ~18.9- to ~158.1-cm, the *S*-ratio shows slight changes in their values and it decreases up to ~185.2 cm, indicating an increase in high-coercivity magnetic contribution (e.g., hematite or goethite). Similar behavior is also observed for HIRM and $B_{1/2}$ parameters, suggesting high-coercivity contribution from ~158.1- to ~185.2-cm depth. In general, the presence of high-coercivity minerals observed in the *S*-ratio, HIRM, and $B_{1/2}$ after ~158.1 cm is indicative of a well-developed soil (yellow layer, probably due to the presence of goethite).

We observe that between ~105- and ~145-cm depth, where archaeological material (number of total pieces) are abundant, the magnetic data presents the most significant variations (Figure 12), mainly in MS and χfd% parameters. Note that the number of total pieces is an average for each level. The increase in-phase in the values of MS and χfd% indicates that the analyzed samples present a contribution of finer magnetic grains, meaning that the material is strongly related to the fired or anthropogenic soil at these depths (e.g., Dalan et al., 2010; Evans & Heller, 2003).

5.4 | Chronology

5.4.1 | Luminescence dating

Seven sediment samples for luminescence dating were collected. The present study investigates OSL on quartz sand. The samples are given in Table 6.

Samples UW 3049, UW 3050, and UW 3051 are related to the archaeological level. Sample UW 3049 was placed in the center of the archaeological layer, whereas sample UW 3050 and UW 3051 represent, respectively, the bottom and the top of the archaeological layer.

The other four samples are related to natural deposition and they are important to understand the site formation processes and chronology. Samples UW 3069 and UW 3063 were collected inside the sandy sterile sediment, and correspond to Beltrão's Layer IV, or the start of the upbuilding of the sandy river terrace. The basal cobble layer, which represents the old river bed, or Beltrão's Layer V, is represented by samples UW 3061 and UW 3062.

Dose rate

The dose rate was measured as described in Section 4.2. Table 7 gives the concentration of the major radionuclides, and the beta dose rate calculated in two ways: (a) Calculated from flame photometry and alpha counting, assuming secular equilibrium and (b) derived directly from beta counting. The two measures are in statistical agreement for all samples, except UW3049. This probably occurred because of some disequilibrium in the U decay chain, not unusual for fluvial sediments. For that sample, the beta dose rate from beta counting was used in age calculation. Total dose rates are given in Table 8. Moisture content was taken as measured, varying from 6% to 7%.

Equivalent dose

The sensitivity of the quartz grains was high, which is typical for many regions of Brazil. Table 9 gives the number of grains measured, those rejected for various reasons, the number of accepted

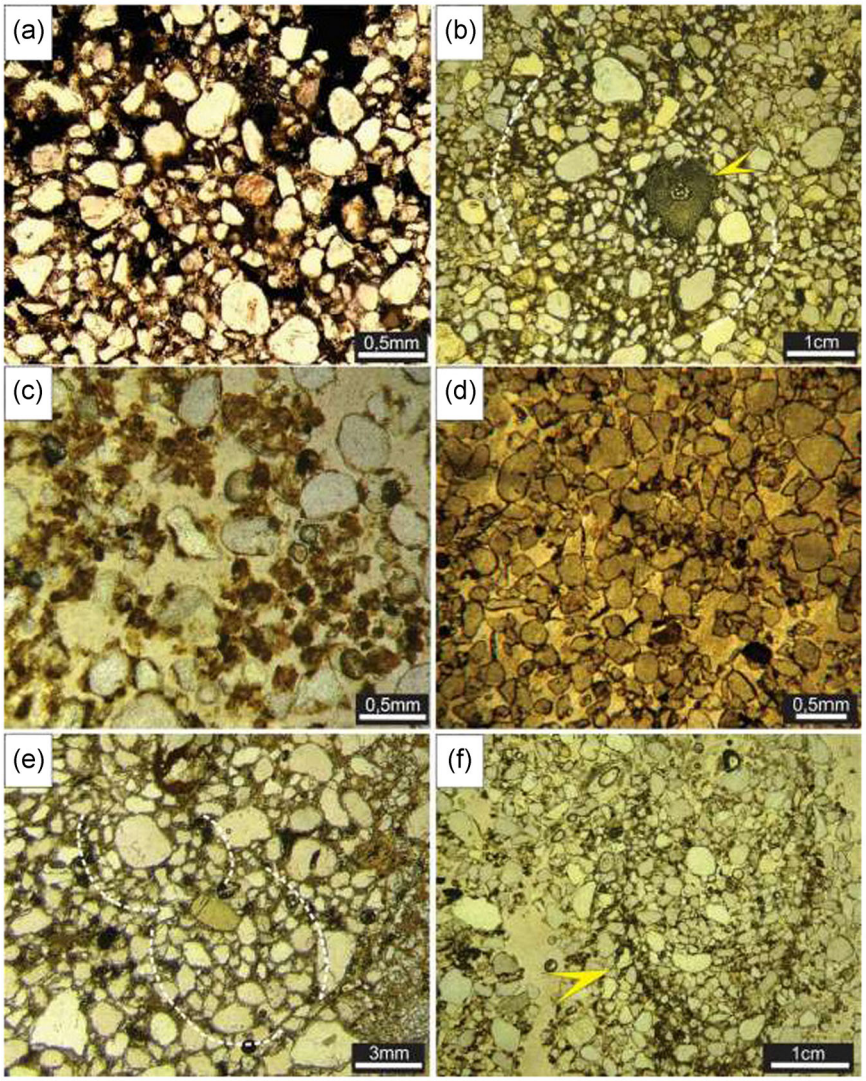

FIGURE 10 (a) Horizon A with micromass composed by organic matter. (b) Root (arrow) associated with crumb structure (dotted line). Note organic matter cementing the grains around the root. (c) Fecal pellets. (d) Horizon without pedological structure composed mainly of quartz grains. (e) Circular structures associated with faunal activity. (f) Meniscate structure produced faunal burrowing [Color figure can be viewed at wileyonlinelibrary.com]

grains, and the ratio of accepted to measured. The average acceptance rate is 28.9%. The high number of failed recycle grains for sample UW3063 is thought due to machine error. Most of these occurred on one disk.

A dose recovery test was done for all samples as a test of procedures. In this test, grains are first set to zero by exposure to the laser and then given a known dose. The SAR procedure is then applied to see if this known dose can be obtained. Table 10 gives the

TABLE 4 Chemical characteristics of the terrace profile

Hor	Depth (cm)	pH (H_2O)	K ($cmol_c\ dm^3$)	Ca	Mg	Al	H + Al	S	CEC	OM (%)	V
A	0–10	5.3	0.21	2.9	0.8	0.1	3.6	3.91	7.51	2.8	52.06
C1	10–32/42	4.7	0.05	0.6	0.3	0.7	3.4	0.95	4.35	1.4	21.84
C2	42–70/80	4.7	0.07	0.5	0.2	0.7	3.4	0.77	4.17	1.2	18.47
C3	80–96/110	4.5	0.11	0.8	0.3	1.1	5	1.21	6.21	1.5	19.48
C4	96–110	4.3	0.09	1.1	0.4	1.3	5.8	1.59	7.39	1.5	21.52
C5	110–160/178	4.4	0.05	0.8	0.3	0.9	3.8	1.15	4.95	1.0	23.23
2C1	160/178–215/236	6.1	0.05	1.1	0.4	-	1.1	1.55	2.65	0.5	58.49
2C2	215/236–241/250	6.3	0.06	1.4	0.5	-	0.9	1.96	2.86	0.7	68.53
2C3	241/250–275	6.3	0.12	1.5	0.7	-	1.0	2.32	3.32	0.9	69.88

Abbreviations: CEC, soil cation exchange capacity; Hor, horizon; OM, organic matter.

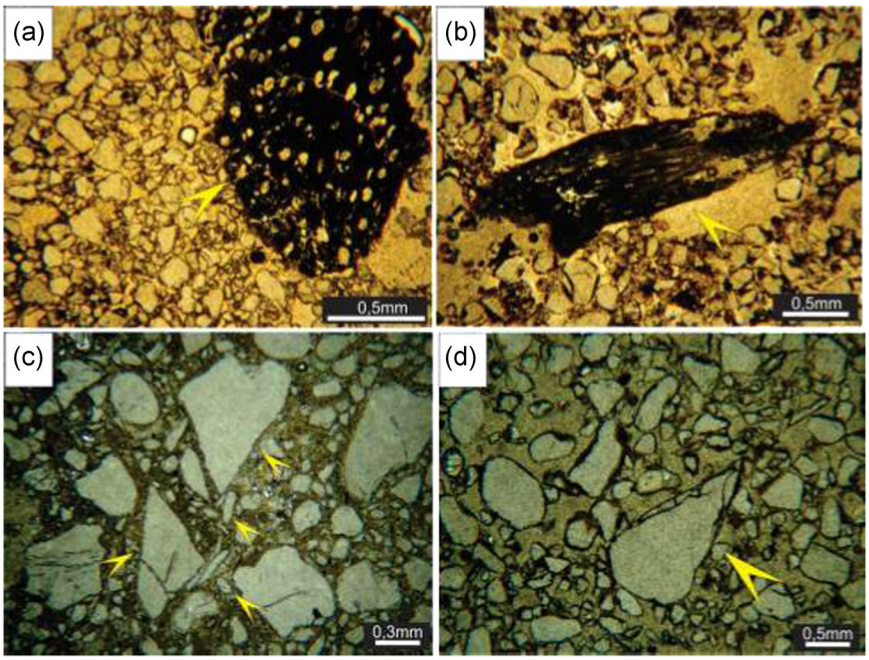

FIGURE 11 (a,b) Charcoal fragments. Note the specific porosity (arrow) associated with the anatomic structures of the plant. (c, d) knapped lithic artifact in soil (arrows). Note the angular shape and the sharp boundary of lithic fragment [Color figure can be viewed at wileyonlinelibrary.com]

ratio of obtained/administered dose and overdispersion for each sample. Dose recovery was excellent and only some of the samples showed any overdispersion. Ten percent overdispersion was assumed to be typical of a single aged sample for the different age models discussed next.

The natural D_e distributions are summarized in Table 11. This gives the number of grains for which a D_e could be derived, the central tendency expressed in terms of the central age model (Galbraith & Roberts, 2012), and the over-dispersion. It also provides the D_e in terms of the minimum age model (Galbraith & Roberts, 2012), which would be appropriate for partially bleached sediments (not uncommon for fluvial sediments). The samples are arranged in stratigraphic order, from top to bottom. Over-dispersion ranges from 34% to 73%, much higher than the 10% assumed from dose recovery for a single-aged sample. This suggests that the samples are composed of different aged grains, either because of mixing or partial bleaching.

Mixing is a strong possibility because the deposits are heavily bioturbated, showing no structure, and having evidence of ant and armadillo burrows. A finite mixture model was thus applied to assess the structure of the data. A finite mixture model (Galbraith & Roberts, 2012) divides the equivalent dose distributions into single-aged components, assuming a normal distribution and, in this case, an overdispersion of 10% as typical for a single-aged sample. Table 12 gives the equivalent dose for each component and the percentage of grains making up that component, again arranging the samples from top to bottom stratigraphically.

OSL ages

By arranging the samples in stratigraphic order, Table 13 compares the ages for the central age model, the minimum age model, and the most common component of the finite mixture model. None of the models produce the correct stratigraphic order, with the bottom two samples being the most discordant. If the minimum age model is used for the top five samples, and either the finite mixture or central age for the bottom two samples, then some semblance of stratigraphic order is obtained. No other combination works.

Figure 13 shows radial graphs of the equivalent dose. Radial graphs plot equivalent dose as a function of precision, with the equivalent dose standardized by the number of standard errors that each value is away from a reference. In this case, the reference is the equivalent dose value that was used to determine the age. Lines drawn from the origin through any point intersect the right-hand axis at the estimated equivalent dose value.

5.4.2 | Radiocarbon dating

Finding charcoal for radiocarbon dating in Alice Boer proved to be a difficult task ever since the first written reports by Beltrão and colleagues. Paradoxically, at the Alice Boer site, the wealth of lithic materials, which suggests a densely occupied area, is not accompanied by macroscopic charcoal fragments. We tried two ways to circumvent this problem: (a) On the one hand, dating of SOM, more specifically the humin fraction which is, supposedly, very stable and not subject to movement across the profile (Gouveia et al., 2002), and (b) dating of millimetric charcoal fragments which were found during the micro-artifact analysis. Seven soil samples and three pieces of charcoal were dated by AMS. One of the charcoal samples was large enough to be detected by the naked eye, but it was close to the surface and, as expected, very recent. The other two charcoal fragments were found in the 1-mm soil fraction, at depths of ca. 105- and 155-cm depth from the surface. Table 14 shows the obtained ages and it is readily apparent that there are strong inconsistencies in the age sequence. We will deal with this phenomenon in the following section.

TABLE 5 Micromorphological description of soil terrace

Horizon (cm)	c/f$_{2\ \mu m}$	Micromass	Coarse material	Relative distribution	Pedofeatures
A/C1 (5–15)	1:1	Dark; undifferentiated	Granular microstructure—40% coarse, 40% mud, 20% voids. Grains: Moderately sorted, subangular to subrounded (medium sand to very fine sand size), cemented by mud and organic matter. Packing voids (very fine sand size)	Open porphyric	Organic matter accumulation; microaggregates of biological origin; biopores; feces; roots and charcoals
C1/C2 (20–38)	1:1	Brown; undifferentiated	Granular microstructure—45% coarse, 40% mud, 15% voids. Grains: Moderately sorted, subangular to subrounded (medium sand to very fine sand size), cemented by mud and organic matter. Chamber voids infilled by mud and organic matter	Open porphyric	Void coatings (very fine sand size); microaggregates of biological origin; biopores; feces; roots and charcoals
C2/C3 (65–78)	1:1	Brown; undifferentiated	Granular microstructure—35% coarse, 30% mud, 35% voids. Grains: Moderately sorted, subangular to subrounded (medium sand to very fine sand size). Channel voids (medium sand size)	Open porphyric	Microartifacts (fine sand size); microaggregates of biological origin; biopores; feces; roots and charcoals
C3/C4/C5 (95–110)	2:1	Brown; weakly speckled b-fabric	Granular microstructure—40% coarse, 30% mud, 30% voids. Grains: Moderately sorted, subrounded (fine to very fine sand size). Channel voids (medium sand size)	Open porphyric	Infillings and amorphous charcoal (very fine sand size); lithic fragments (0.6–1.2mm)
2C1 (155–173)	3:1	Brown; weakly speckled b-fabric	Simple granular microstructure—45% coarse, 20% mud, 35% voids. Grains: Moderately sorted, subrounded (fine to very fine sand size). Packing voids (very fine sand size) and channels voids medium sand size)	Chitonic/Gefuric	Roots residues (medium sand size), amorphous charcoal (very fine sand size) and iron oxide nodule (coarse sand size); lithic fragments (2 mm)
2C1 (158–178)	4:1	Weakly speckled b-fabric	Simple granular microstructure—55% coarse, 10% mud, 35% voids. Grains: Moderately sorted, subrounded (fine to very fine sand size). Packing voids interconnected (fine to very fine sand size)	Chitonic/Gefuric	Amorphous charcoal and iron nodules (very fine sand size)
2C2/2C3 (255–270)	4:1	Undifferentiated; weakly speckled b-fabric	Simple granular microstructure—55% coarse, 10% mud, 35% voids. Grains: Moderately sorted, subrounded (medium to very fine sand size). Packing voids interconnected (fine sand size)	Chitonic/Gefuric	Amorphous charcoal (very fine sand size) and iron nodules (fine and very fine sand size)

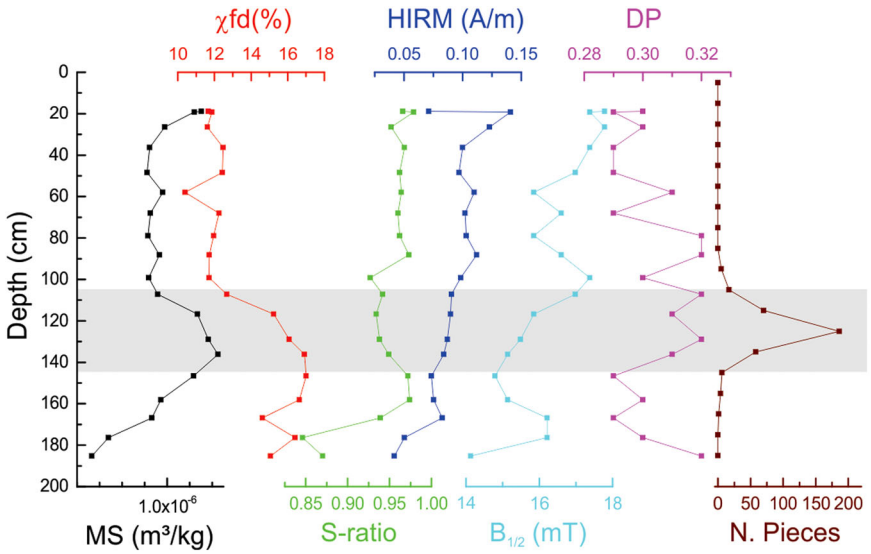

FIGURE 12 Magnetic parameters in function of depth: Low-field magnetic susceptibility (MS), frequency-dependent MS (χfd%), soft-ratio (*S*-ratio), high-coercivity isothermal remanent magnetization (HIRM), median destructive field (B1/2), and the dispersion parameter (DP). We also compare the magnetic parameters with the total number of pieces average observed at each level interval [Color figure can be viewed at wileyonlinelibrary.com]

TABLE 6 Vertical positioning of the samples in the west profile, 1979 excavation

Lab sample #	Sample ID	Z/depth (m)[a]
UW3051	OSL C	3.28/1.15
UW3049	OSL A	3.01/1.45
UW3050	OSL B	2.70/1.75
UW3069	#129	2.42/2.03
UW3063	#128	1.90/2.55
UW3061	#51	1.47/2.97
UW3062	#127	1.40/3.05

Abbreviation: OSL, optically stimulated luminescence.

[a]Z is the elevation above the current river level. Depth is the vertical distance below the current surface, which, however, has been disturbed by previous excavation.

6 | DISCUSSION

The comparison between the data gathered by our interventions and previous publications suggest that the radiocarbon samples obtained by Beltrão et al. (1974) were collected on the "1965" excavation area (Figure 4), 10-m south from the location we dated, whereas the TL samples came from the "1980" excavation, about the same distance. However, we think that the ages we obtained can be extrapolated to the other excavation areas without a problem; we found the same sequence of layers/colors described by previous authors. The archaeological layer we detected on the west profile of the "1979" excavation can be securely correlated to Beltrão's "Layer III" or "Layer 6 and 7" according to Poupeau, Cunha, et al. (1984; see Figure 5). Poupeau, Souza, et al. (1984) was able to correlate the "1979" and "1980" excavation stratigraphy with the original "1965" stratigraphy, so we can surmise that the site shows a somewhat continuous archaeological layer, whose thickness can be variable.

If we take the 10 levels in which "Layer III" was subdivided after the "1965" excavation (Table 1), we can suppose that the archaeological layer was 1-m thick at that point, whereas in our excavation it showed no more than 50 cm. Therefore, it is possible that the archaeological layer shows an increase in thickness toward the river.

6.1 | Site chronology and formation processes

The minimum luminescence ages presented in Table 11 are the youngest the samples could be, and can be justified either by partial bleaching or, alternatively, by postdepositional mixing bringing older

TABLE 7 Radioactivity information

Sample	^{238}U (ppm)	^{233}Th (ppm)	*K* (%)	Beta dose rate (Gy/ka)	
				β-counting	*α*-counting/flame photometry
UW3051	0.50 ± 0.07	3.08 ± 0.61	0.39 ± 0.01	.53 ± .05	.48 ± .02
UW3049	1.93 ± 0.15	6.43 ± 1.02	0.41 ± 0.01	.54 ± .05	.80 ± .04
UW3050	1.14 ± 0.10	3.54 ± 0.67	0.33 ± 0.02	.45 ± .05	.53 ± .03
UW3069	0.69 ± 0.06	0.87 ± 0.35	0.44 ± 0.01	.57 ± .06	.49 ± .02
UW3063	0.40 ± 0.06	3.11 ± 0.63	0.62 ± 0.01	.74 ± .07	.65 ± .02
UW3061	0.68 ± 0.06	1.90 ± 0.44	0.30 ± 0.03	.43 ± .07	.40 ± .03
UW3062	0.41 ± 0.07	4.21 ± 0.79	0.51 ± 0.01	.67 ± .06	.60 ± .03

TABLE 8 Total dose rates (Gy/ka)

Sample	α	β	γ	Cosmic	Total
UW3051	.01 ± .01	.39 ± .02	0.28 ± 0.03	0.17 ± 0.03	0.84 ± 0.05
UW3049	.01 ± .01	.43 ± .03	0.58 ± 0.05	0.17 ± 0.03	1.19 ± 0.07
UW3050	.01 ± .01	.36 ± .02	0.35 ± 0.03	0.16 ± 0.03	0.88 ± 0.05
UW3069	.01 ± .01	.47 ± .02	0.21 ± 0.02	0.16 ± 0.03	0.84 ± 0.04
UW3063	.01 ± .01	.55 ± .02	0.33 ± 0.01	0.15 ± 0.03	1.03 ± 0.04
UW3061	.01 ± .01	.32 ± .03	0.23 ± 0.02	0.14 ± 0.03	0.69 ± 0.05
UW3062	.01 ± .01	.49 ± .03	0.35 ± 0.04	0.14 ± 0.03	0.99 ± .05

TABLE 9 Acceptance rates

Sample	*N*	No signal	Failed recycle	Too high	Recuperation/ zero dose	Feldspar	Accepted	Rate (%)
UW3051	384	153	22	9	5	2	193	50.3
UW3049	384	228	20	7	7	10	112	29.2
UW3050	385	235	13	20	2	5	110	28.6
UW3069	386	225	16	9	6	4	126	32.6
UW3063	387	70	113	57	0	0	147	38.0
UW3061	584	445	13	22	6	1	97	16.7
UW3062	579	376	32	50	6	8	107	18.5
Total	3089	1732	229	174	32	30	892	28.9

Note: "No signal" refers to grains that lacked a measurable signal, as judged by an error greater than 30% on the test dose or a natural signal that was not at least three standard deviations above background. The other criteria for rejection were for those grains where the designated criterion was the only problem. "Failed recycle" refers to grains where the recycle ratio did not fall within 0.8 and 1.2. "Recuperation" refers to grains where the signal from a zero dose was more than 10% of the natural signal. "Too high" refers to grains where the natural signal was larger than the signal from the highest regeneration dose and thus did not intersect the growth curve. "Zero dose" refers to grains where the derived equivalent dose was not significantly different from zero. "Feldspar" refers to grains where the signal lost intensity due to an infrared exposure. All grains falling under these criteria were rejected for analysis.

sediments up. If, on the contrary, the youngest grains represent turbation processes bringing young grains down, then the minimum age would be an underestimate. In that case, maybe the second youngest component of the finite mixture model would represent the depositional age, but this yields ages from 10 to 30 ka for the top five samples. This is hard to reconcile with the ages for the bottom two samples and seems too old for the archaeological context. More likely, mixing preferentially brought older grains up and this would not affect minimum age determinations. Ants are known to preferentially move older grains up (Araujo, 2013). The minimum age

TABLE 10 Dose recovery data

Sample	*N*	Obtained/ administered	Overdispersion (%)
UW3051	42	0.99 ± 0.02	9.9 ± 2.5
UW3049	46	1.02 ± 0.01	0
UW3050	35	0.98 ± 0.02	0
UW3069	44	1.00 ± 0.02	7.3 ± 1.8
UW3063	62	1.02 ± 0.03	13.9 ± 2.4
UW3061	22	1.01 ± 0.02	0
UW3062	19	1.01 ± 0.03	3.5 ± 4.4

TABLE 11 D_e (Gy) distributions

Sample	*N*	Central age D_e (Gy)	σ_b (%)	Minimum age D_e (Gy)
UW3051	193	10.84 ± 0.41	47.5 ± 2.9	5.27 ± 0.26
UW3049	112	13.55 ± 0.80	58.1 ± 4.3	5.59 ± 0.40
UW3050	110	22.03 ± 1.30	57.6 ± 4.4	7.11 ± 0.52
UW3069	126	26.09 ± 1.15	44.2 ± 3.4	12.38 ± 0.88
UW3063	147	35.01 ± 1.18	33.7 ± 2.7	18.62 ± 1.10
UW3061	97	23.88 ± 1.98	73.0 ± 6.3	5.07 ± 0.59
UW3062	107	28.17 ± 1.44	44.6 ± 4.0	11.12 ± 0.88

TABLE 12 Finite mixture model

	Component 1		Component 2		Component 3		Component 4		Component 5	
Sample	D_e (Gy)	%	D_e (Gy)	%	D_e (Gy)	%	D_e (Gy)	%	D_e (Gy)	%
UW3051	5.00 ± 0.22	11	8.61 ± 0.46	28	12.2 ± 0.36	51	23.6 ± 1.25	7	42.2 ± 4.24	2
UW3049	6.02 ± 0.29	17	11.3 ± 0.32	48	20.8 ± 0.90	20	35.8 ± 1.72	15		
UW3050	8.37 ± 0.32	21	18.2 ± 0.83	22	34.2 ± 0.80	57				
UW3069	8.64 ± 0.89	7	17.3 ± 0.73	24	29.9 ± 0.96	49	43.6 ± 21.2	20		
UW3063	14.5 ± 0.77	8	33.6 ± 1.14	64	49.1 ± 3.49	28				
UW3061	4.27 ± 0.39	10	14.0 ± 1.21	18	27.6 ± 1.38	42	48.9 ± 2.12	30		
UW3062	10.2 ± 0.59	14	27.1 ± 1.01	54	45.8 ± 2.06	31				

model does not work for the bottom two samples (UW 3061 and UW 3062), making them more recent than samples higher in the stratigraphy. These samples were collected inside the basal cobble layer, and therefore the sediment was most probably deposited along the bottom of the ancient river channel. They were probably subject to partial bleaching, accounting for the above 40 ka grains found in these and other samples. The presence of younger grains in these samples, however, must be due to the downward postdepositional movement of the overlying sands. Both samples are close to the bedrock (the clayey Corumbataí Formation, Upper Permian/Lower Triassic age), so there is not much room for postdepositional movement of sand grains upwards. Considering these factors, it is reasonable to accept the minimum ages for the upper five samples, which were taken from well-drained, sandy riverine sediments. They most probably were subject to a predominantly upward movement of older sand grains through the action of ants, termites, and other burrowing animals. On the contrary, for the two lower samples, placed inside the cobble layer, the downward migration of sand particles seems more likely for three reasons: (1) proximity of the bedrock; (2) gravity, which allows the overlying sand grains to percolate between the cobbles; and (3) the proximity of the water table, which prevents any strong action of burrowing animals. In this case, the most common component of the finite mixture model seems a better estimate of the equivalent dose, which makes them stratigraphically consistent (Table 13).

We dated a sand-sized (1 mm) fragment of charcoal (sample ALB 12; Tables 14 and 15), with an age of 8471 ± 48 cal BP. The positioning of this piece is very close to OSL sample UW 3051 (top of the archaeological layer). The OSL age is 6290 ± 520 BP. As the charcoal fragment is very small, it could be transported upwards by ants or termites (Araujo, 2013), and we tend to consider this radiocarbon age as a maximum age for the top of the layer. The OSL age is considered more reliable. There is a very good agreement between sample UW 3050 and ^{14}C sample ALB 07 (another 1-mm charcoal fragment). The OSL age is 8110 ± 80 BP, whereas the cal ^{14}C age is 8013 ± 42 calBP. These samples correspond to the lower limit of the archaeological layer, and therefore, can be considered as the maximum age for the site. Sample UW 3049 was taken in the middle of the archaeological layer. There is no charcoal to compare with, but the age is too young (4710 ± 450 BP), compared to the others from this layer. Perhaps we have the effect of a collapsed armadillo burrow or root, in this case, as both bioturbation agents are abundant on the site.

TABLE 13 Luminescence samples and obtained ages

Lab sample #	Sample ID	depth (m)	Central age model	Minimum age model	Finite mixture model
UW3051	OSL C	1.15	12.9 ± 0.99	6.29 ± 0.52	14.6 ± 1.06
UW3049	OSL A	1.45	11.4 ± 1.00	4.71 ± 0.45	9.48 ± 0.67
UW3050	OSL B	1.75	25.1 ± 2.24	8.11 ± 0.80	39.0 ± 2.76
UW3069	#129	2.03	31.0 ± 2.26	14.7 ± 1.35	35.5 ± 2.36
UW3063	#128	2.55	34.1 ± 2.04	18.2 ± 1.40	32.8 ± 1.96
UW3061	#51	2.97	34.4 ± 3.83	7.32 ± 1.01	20.2 ± 2.31
UW3062	#127	3.05	28.5 ± 2.30	11.3 ± 1.14	27.5 ± 2.00

Note: All samples were collected from the west profile of the 1979 excavation and placed in stratigraphic order, from upper to lower.

Abbreviation: OSL, optically stimulated luminescence.

*"Z" is the elevation above the current river level, whereas "depth" is the vertical distance below the current surface, which, however, has been disturbed by previous excavations.

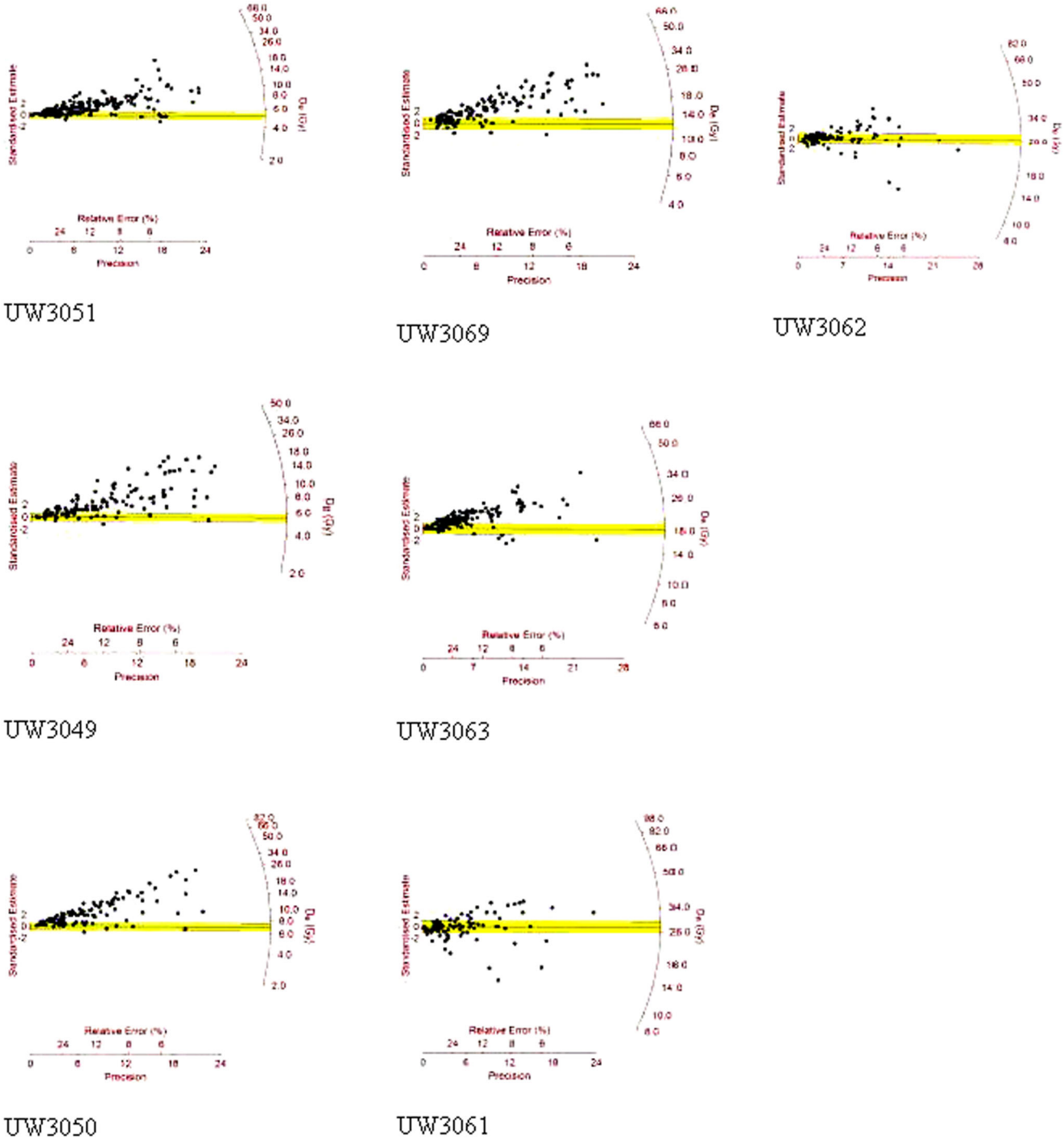

FIGURE 13 Radial graphs, where the equivalent dose is standardized by the number of standard errors each value is away from a reference, plotted against precision [Color figure can be viewed at wileyonlinelibrary.com]

As already mentioned, samples UW 3069 and UW 3063 were collected in an archaeologically sterile sandy sediment, and correspond to Beltrão's Layer IV, or the start of the upbuilding of the sandy river terrace. The basal age (UW 3063) is 18,150 ± 1400 BP; the top age is 14,680 ± 1350 BP.

Finally, the basal cobble layer, which represents the old river bed, or Beltrão's Layer V, was dated by OSL at around 20–30 ka (samples UW 3061 and UW 3062).

The microartifacts (Figure 8) do not mirror exactly the vertical distribution of larger pieces (Figure 6). This is expected for two reasons: First, the vertical positioning of large pieces is a mean of their vertical distribution across the whole profile, whereas microartifacts were collected along a narrow, vertical band. Second, microartifactual data must always be regarded as providing different, complementary, and not necessarily supplementary information (Dunnell & Stein, 1989). In this case, microartifacts could indicate the

TABLE 14 Radiocarbon ages for Alice Boer, calibrated according to Reimerr et al. (2009) INTCAL 09 calibration curve, as given in Beta Analytic report

Sample	Lab ID	Unit	Depth (cm)	Z	Sample type	$^{13}C/^{12}C$ ratio (0/00)	^{14}C standard	Cal BP 2 sigma
ALB 22	Beta 315477	West Profile 1979	0–10	4328	Soil–humin fraction	−24.5	101 ± 9	Modern
ALB 22 charcoal	Beta 316478	West Profile 1979	0–10	4328	Charcoal	−26.1	70 ± 30	Cal BP 260–220 and Cal BP 140–30
ALB 12[a]	Beta 320199	West Profile 1979	100–110	3358	Charcoal 1-mm fraction	N/A	7680 ± 40	Cal BP 8550–8400
ALB 11[a]	Beta 312262	West Profile 1979	110–120	3262	Soil–humin fraction	−23.8	1950 ± 30	Cal BP 1980–1980 and Cal BP 1970–1960 and Cal BP 1950–1860 and Cal BP 1850–1830
ALB 10[a]	Beta 312261	West Profile 1979	120–130	3141	Soil–humin fraction	−23.1	2080 ± 30	Cal BP 2130–1990 and Cal BP 1960–1950
ALB 9[a]	Beta 312260	West Profile 1979	130–140	3068	Soil–humin fraction	−22.9	1490 ± 30	Cal BP 1410–1310
ALB 8[a]	Beta 312259	West Profile 1979	140–150	2964	Soil–humin fraction	−22.6	2580 ± 30	Cal BP 2750–2710 and Cal BP 2630–2620
ALB 7[a]	Beta 312258	West Profile 1979	150–160	2849	Soil–humin fraction	−22.1	2970 ± 30	Cal BP 3250–3070
ALB 07 charcoal[a]	Beta 320198	West Profile 1979	150–160	2849	charcoal 1-mm fraction	−26.3	7200 ± 40	Cal BP 8150–8140 and Cal BP 8130–8120 and Cal BP 8100–8100 and Cal BP 8050–7950
ALB 50	Beta 315478	T1 excav. 1979 central	basal cobble layer	1515	Soil–humin fraction	−22.6	1430 ± 30	Cal BP 1370–1290

[a]Samples associated with archaeological materials.

TABLE 15 Compilation of all obtained ages and their vertical positioning

Sample	Unit	Depth (cm from top soil)	*Z* (mm above river)	Sample type	Cal years BP
ALB 22	East Profile 1979	0–10	4328	*Soil–humin fraction*	144 ± 91
ALB 22 charcoal	East Profile 1979	0–10	4328	Charcoal	133 ± 93
ALB 12	East Profile 1979	100–110	3358	Charcoal 1-mm fraction	8471 ± 48
UW 3051	East Profile 1979	115	3280	OSL	6290 ± 520
ALB 11	East Profile 1979	110–120	3262	*Soil–humin fraction*	1903 ± 36
ALB 10	East Profile 1979	120–130	3141	*Soi–humin fraction*	2053 ± 48
ALB 9	East Profile 1979	130–140	3068	*Soil–humin fraction*	1369 ± 34
UW 3049	East Profile 1979	145	3012	OSL	4710 ± 450
ALB 8	East Profile 1979	140–150	2964	*Soil–humin fraction*	2724 ± 30
ALB 7	East Profile 1979	150–160	2849	*Soil–humin fraction*	3133 ± 51
ALB 07 charcoal	East Profile 1979	150–160	2849	Charcoal 1-mm fraction	8013 ± 42
UW 3050	East Profile 1979	175	2699	OSL	8110 ± 80
UW 3069	East Profile 1979	203	2144	OSL	14760 ± 1350
UW 3063	East Profile 1979	255	1895	OSL	18,200 ± 1400
ALB 50	T1 excavation 1979 central	basal cobble layer	1515	*Soil–humin fraction*	1329 ± 28
UW 3061	East Profile 1979	297	1472	OSL	29,710 ± 3530
UW 3062	East Profile 1979	305	1395	OSL	27,500 ± 2000

Note: Humin AMS ages are in italics. To ease the comparison, calibrated ages here were obtained using CalPal program, INTCAL13 calibration curve (Weninger et al., 2012).

possible presence of an upper occupation level, not detected by larger archaeological materials, between 50- and 90-cm depth. This possibility is strengthened by Poupeau's observations (Poupeau, Cunha, et al., 1984), when he observed lithics above "Layer III," on the upper colluvial material (see Figure 5).

Another important observation is related to the vertical positioning of the charcoal microscopic fragments, since it appears that they are not directly related to the human occupation at the site. This was also observed in the micromorphological thin sections in which charcoal appears across the profile. Hence, there is the possibility that the microscopic charcoal was carried by the river from upstream sources and deposited at the site. This can be an alternative explanation for the discrepant age obtained on a small charcoal particle, sample ALB 12 (see Table 15).

When we compare our chronology with the one obtained by previous works and presented in Table 1, it is possible to perceive several incongruences. If we keep in mind that the 10 levels presented in Table 1 do not correspond to the whole site stratigraphy, but only to the 1-m-thick archaeological layer ("Layers IIIa and IIIb" or "Layers 6 and 7"), it appears that all TL ages from levels 1 to 7 are too young. The original profile published by Beltrão (1974, p. 219) does not have a graphic scale, but if layers IIIa and IIIb are 1-m thick, we can estimate that they were covered by at least 1 m of sediment. This means that ages in "level 1," purportedly dating about 2 ka, were already 1-m deep. At this depth, our ages are about 6.3 ka. The same can be said about radiocarbon ages down to level 8. All radiocarbon ages were discrepant with the TL ages, except for the intervals between levels 5 and 7, where they converge to approximately 6–6.3 ka, again, too young. On the contrary, the TL ages from levels 8 to 10, in addition to present very high errors, seem too old when compared to our data. Lastly, the 14,200 ± 1150 ^{14}C age obtained in the bottom also shows a very large error and does not match any of the ages we obtained for the bottom of the archaeological layer.

Given our chronological results, which tend to dismiss great antiquity for the site, it is important to notice that in terms of the lithic industry, Alice Boer can be related to older manifestations (see Araujo et al., 2020). For instance, there is a strong material culture similarity with the Caetetuba site (Moreno de Sousa, 2019; Troncoso et al., 2016), dated to 10.9 ka and located 90-km west of Alice Boer.

6.2 | Humin fraction AMS dating: Not a reliable chronological tool

It is important to note that all ages obtained by means of SOM, specifically the humin fraction, which is considered by several authors as the more stable, unmovable, OM component (Gouveia et al., 2002; Jull et al., 2004; Pessenda et al., 2001, 2004; Riris et al., 2018; Watling et al., 2017), seems absolutely unsuitable for dating sandy tropical soils. Future work should be directed to check if this is also

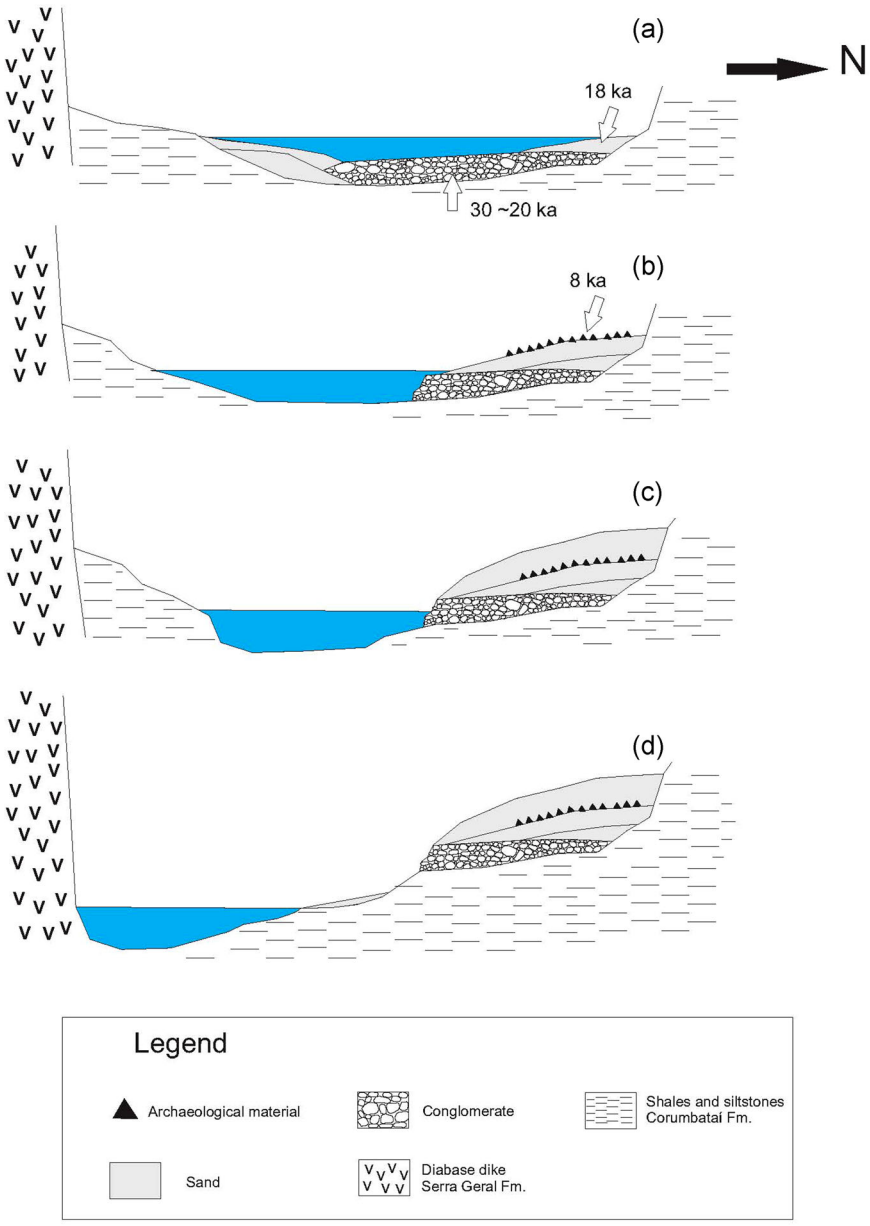

FIGURE 14 Model of the site formation processes operating at Alice Boer. (a) Deposition of a cobble layer related to the former river bed, ca. 30–20 ka, and initial deposition of the sandy terrace at ca. 18 ka. (B) Continuity of the sandy deposition by overbank deposits and human occupation ca. 8 ka. (c) Overbank deposition continues and covers human occupation. (d) River migrates southwards, the channel deepens, and overbank deposition stops [Color figure can be viewed at wileyonlinelibrary.com]

true for clayey soils. The humin ages are always much younger than either charcoal or OSL ages (Table 15). The dating lab did not detect any problem with the samples, stating in the report that they "provided plenty of carbon for accurate measurements and all the analyses proceeded normally" (Beta Analytic Inc., 2012). We note here that the amount of charcoal per se is not a guarantee of accuracy.

The only correspondence between humin and charcoal occurs in the first centimeters of the profile (paired samples ALB 22 and ALB 22 charcoal). Between 1.0- and 1.4-m depth, humin ages that should be at least 6 ka showed ages around 2 ka. Another paired sample (ALB 07 and ALB 07 charcoal) placed 1.5-m-deep show ages of 8 ka for charcoal and 3 ka for humin. Moreover, we obtained a humin age of 1.3 ka for Layer V (sample ALB 50), which is undoubtedly of the Pleistocene age, bracketed between 18 and 30 ka. This sample is close to the water table, and this very recent age suggests that humin also travels horizontally, following the subterranean water flow. This last observation is of importance regarding the possibility that young OM contamination can severely compromise the ages of charcoal fragments close to the water table.

7 | CONCLUSIONS

Alice Boer site was heavily occupied and can be considered as an important site for the understanding of the early human occupation of inner Southeastern Brazil. However, its age can be securely considered as not older than 8 ka. Nevertheless, the lithic industry of Alice Boer can be related to an older chronological range.

Our model for the formation processes of the Alice Boer site can be summarized as follows (Figure 14):

(1) At ca. 30–20 ka, the Cabeça river had its channel flowing where the site is located, depositing coarse sediments (cobbles, pebbles, coarse sand; Figure 14a).
(2) The river migrates toward the south and the old channel deposits are exposed; sand bars start to accumulate over the cobble layer. The gap between the top of the cobble layer and the overlying sandy sediments (at least 2 ka) suggests several erosion events, perhaps due to the proximity of the river. At ca. 18 ka, the river is distant and deep enough to allow the deposition of a sandy deposit forming a beach (Figure 14b).
(3) The upbuilding of the sandy overbank deposits continue from 18 ka until human occupation, ca. 8 ka and after, covering the archaeological deposits (Figure 14c). Therefore, there was running water involved in the sediment upbuilding process. *This factor can be invoked to explain the lack of charcoal inside the sediment*. Large charcoal particles are light enough to be washed away during seasonal riverine overflow, as suggested by the results of the excavation unit close to the river. Moreover, the magnetic data suggests that fire activities were significant in the main archaeological layer (Figure 12). We tend to dismiss the possibility that bioturbation was responsible for the destruction of charcoal fragments or its reduction to sand-sized particles as we studied a Paleoindian site in the same region (Lagoa do Camargo), also in sandy soil, showing abundant charcoal particles (Araujo et al., 2017).
(4) The river deepens its channel and the deposition of sand stops (Figure 14d). Pedogenetic processes start to operate and organic matter from the A horizon accumulates and percolates through the profile. If we take into account the ages obtained by humin (not taking into account their vertical position, of course), we can say that this process starts around 3 ka (sample ALB 7).

Regarding soil AMS dating, our observations strongly suggest that humin percolates downwards and laterally with water, and is much less reliable as a chronological marker than commonly thought, at least in sandy soils in tropical settings. Therefore, paleoenvironmental reconstructions and archaeological dating based on humin alone should be viewed with utmost caution. As we observed elsewhere (Araujo et al., 2017), the dating of archaeological sites in tropical soils demands the use of more than a single method. In this regard, we maintain that luminescence must always be carried together with radiocarbon dating to address complex issues regarding sediment mixing, carbon contamination, and other site formation processes.

ACKNOWLEDGMENTS

We would like to thank Dr. Antonio Carlos Sarti (EACH/USP) for helping and supporting our work in several instances, Dr. José Eduardo Zaine (UNESP/Rio Claro) for sharing valuable data about the geology of the area, as well for discussions about site formation processes. To Dr. João Messeti for granting access to his property. Mr. João Boer (*in memoriam*) also provided helpful information about the site. Dr. Paulo C. Giannini kindly granted the use of the Laboratory of Sedimentology, Institute of Geosciences, University of São Paulo. We also thank the two anonymous reviewers for improving the quality of the paper. This study was supported by FAPESP, grants 2009/54.720-9, 2013/13.794-5, and 2016/23.584-6 (AGMA), and CNPq, grants 300339/2008-9, 302024/2019-0 (AGMA), and 308629/2015-9, 307951/2018-9 (FSBL). Scientific editing by Vance Holliday.

CONFLICT OF INTERESTS

The authors declare that there are no conflict of interests.

AUTHOR CONTRIBUTIONS

Conceptualization, funding acquisition, investigation, methodology, project administration, and writing the original draft: Astolfo G. de Mello Araujo. OSL dating methodology, writing the original draft and lab processing: James K. Feathers. Investigation, writing the original draft, magnetometry analysis and lab processing: Gelvam A. Hartmann. Investigation, writing the original draft, pedological analysis and lab processing: Francisco S. B. Ladeira. Pedological analysis, figures and lab processing: Éverton V. Valezio. Pedological analysis and lab processing: Diego L. Nascimento. Microartifact analysis and methodology: Olivia Ricci. Magnetometry analysis and lab processing: Victor J. de Oliveira Marum. Magnetometry analysis and lab processing: Ricardo I. Ferreira da Trindade.

DATA AVAILABILITY STATEMENT

The data that support the findings of this study are openly available in the Humanities Commons Repository at https://doi.org/10.17613/x5rv-ax34, for the lithic analysis and spatial positioning of the pieces and https://doi.org/10.17613/dk11-c902 for the microartifact data.

ORCID

Astolfo G. de Mello Araujo http://orcid.org/0000-0002-0349-1226
James K. Feathers https://orcid.org/0000-0002-1309-6131
Gelvam A. Hartmann https://orcid.org/0000-0001-6078-3893
Francisco S. B. Ladeira https://orcid.org/0000-0002-9990-2332
Éverton V. Valezio https://orcid.org/0000-0003-3587-1503
Diego L. Nascimento https://orcid.org/0000-0002-5140-7471
Victor J. de Oliveira Marum https://orcid.org/0000-0002-7187-9310
Ricardo I. Ferreira da Trindade https://orcid.org/0000-0001-9848-9550

REFERENCES

Araujo, A. G. M., Moreno de Sousa, J., Correa, L., Feathers, J., & Okumura, M. M. (2020). The rise and fall of Alice Boer site: A reassessment of a purported pre-Clovis site. *Geoarchaeology — An International Journal*. Manuscript in press.
Angelucci, D. E. (2010). The recognition and description of knapped lithic artifacts in thin section. *Geoarchaeology*, *25*, 220–232. https://doi.org/10.1002/gea.20303
Araujo, A. G. M. (1995). Peças que descem, peças que sobem e o fim de Pompéia: Algumas observações sobre a natureza flexível do registro

arqueológico. *Revista do Museu de Arqueologia e Etnologia*, *5*, 3–25. https://doi.org/10.11606//inss.2448-1750.revmae.1995.109215

Araujo, A. G. M. (2013). Bioturbation and the upward movement of sediment particles and archaeological materials: Comments on Bueno et al. *Journal of Archaeological Science*, *40*, 2124–2127. https://doi.org/10.1016/j.jas.2012.12.035

Araujo, A. G. M. (2015). On vastness and variability: Cultural transmission, historicity, and the Paleoindian record in eastern South America. *Anais da Academia Brasileira de Ciências*, *87*, 1239–1258. https://doi.org/10.1590/0001-3765201520140219

Araujo, A. G. M., & Feathers, J. K. (2008). First notice of open-air Paleoamerican sites at Lagoa Santa: Some geomorphological and paleoenvironmental aspects, and implications for future research. *Current Research in the Pleistocene*, *25*, 27–29.

Araujo, A. G. M., Paisani, J. C., Schrage, T. J., Feathers, J. K., Hartmann, G. A., & Ricci, O. (2017). The "Lagoa do Camargo 1" Paleoindian site: Some implications for tropical geomorphology, pedology, and paleoenvironments in Southeastern Brazil. *Geoarchaeology*, *32*, 662–677. https://doi.org/10.1002/gea.21628

Araujo, A. G. M., Strauss, A. M., Feathers, J. K., Paisani, J. C., & Schrage, T. J. (2013). Paleoindian open-air sites in tropical settings: A case study in formation processes, dating methods, and paleoenvironmental models in Central Brazil. *Geoarchaeology*, *28*, 195–220. https://doi.org/10.1002/gea.21442

Bate, L. F. (1990). Culturas y modos de vida de los cazadores recolectores en el poblamiento de América del Sur. *Revista de Arqueología Americana*, *2*, 89–153.

Beattie, O. B., & Bryan, A. L. (1984). A fossilized calotte with prominent browridges from Lagoa Santa, Brazil. *Current Anthropology*, *25*, 345–346. https://doi.org/10.1086/203143

Bednarik, R. G. (1989). On the Pleistocene settlement of South America. *Antiquity*, *63*, 101–111. https://doi.org/10.1017/S0003598X0007561X

Beltrão, M. C. (1974). Datações arqueológicas mais antigas do Brasil. *Anais da Academia Brasileira de Ciências*, *46*, 211–251.

Beltrão, M. C. (2000). *Ensaio de Arqueologia. Uma Abordagem Transdisciplinar*. ZIT Gráfica e Editora.

Beltrão, M. C. (2008). *Le Peuplement de l'Amerique du Sud: Essai d'Archeologie, une Approche Interdisciplinaire*. Riveneuve Editions.

Beltrão, M. C., & Andrade Lima, T. (1986). Projeto Central, Bahia: Os zoomorfos da Serra Azul e da Serra de Santo Ignácio. *Revista do Patrimônio Histórico e Artístico Nacional*, *21*, 147–156.

Beltrão, M. C., Danon, J., Enriquez, C. R., Poupeau, G., & Zuleta, E. (1982). On the arrival of men in America: Dating by thermo-luminescence of heated cherts from archaeological site Alice Boer (Brasil). *Comptes Rendus De L'Academie des Sciences Serie II*, *295*, 629–632.

Beltrão, M. C., Enriquez, C. R., Danon, J., Zuleta, E., & Poupeau, G. (1983). *Thermoluminescence dating of burnt cherts from the Alice Boer site Brazil)* (Report No. CBPF-NF-004/83). Centro Brasileiro de Pesquisas Fisicas.

Beta Analytic Inc. (2012). *Radiocarbon dating results for samples ALICE BOER07, ALICE BOER08, ALICE BOER09, ALICE BOER11*. Ms. in possession of the authors.

Boëda, E., Clemente-Conte, I., Fontugne, M., Lahaye, C., Pino, M., Felice, G. D., Guidon, N., Hoeltz, S., Lourdeau, A., Pagli, M., & Pessis, A. M. (2014). A new Late Pleistocene archaeological sequence in South America: The Vale da Pedra Furada (Piauí, Brazil). *Antiquity*, *88*, 927–941. https://doi.org/10.1016/S0277-3791(99)00046-3

Braje, T. J., Erlandson, J. M., Rick, T. C., Davis, L., Dillehay, T., Fedje, D. W., Froese, D., Gusick, A., Mackie, Q., McLaren, D., Pitblado, B., Raff, J., Reeder-Myers, L., & Waters, M. (2020). Fladmark+ 40: What have we learned about a potential Pacific Coast peopling of the Americas? *American Antiquity*, *85*(1), 1–21.

Bryan, A., & Beltrão, M. C. (1978). An early stratified sequence near Rio Claro, East Central São Paulo State, Brazil, *Early man in America from a circum-Pacific perspective* (pp. 303–305). University of Alberta.

Bullock, P., Fedoroff, N., Jongerius, A., Stoops, G., & Tursina, T. (1985). *Handbook for soil thin section description*. Wayne Research Publishing.

Bøtter-Jensen, L., & Mejdahl, V. (1988). Assessment of beta dose-rate using a GM multi-counter system. *Nuclear Tracks and Radiation Measurements*, *14*, 187–191. https://doi.org/10.1016/1359-0189(88)90062-3

Calderón, G. A., & Politis, G. (1989). Nuevos datos para un viejo problema: Investigación y discusiones en torno del poblamiento de América del Sur. *Boletin Museo del Oro*, *23*, 3–45.

Cunha, L. M. (1994). Le Site d'Alice Boer (Bresil). *L'Anthropologie*, *98*(1), 110–127.

Dalan, R., & Banerjee, S. K. (1998). Solving archaeological problems using techniques of soil magnetism. *Geoarchaeology*, *13*, 3–36. https://doi.org/10.1002/(SICI)1520-6548(199801)13:1%3C3::AID-GEA2%3E3.0.CO;2-9

Dalan, R. A., de Vore, S. L., & Clay, R. B. (2010). Geophysical identification of unmarked historic graves. *Geoarchaeology*, *25*, 572–601. https://doi.org/10.1002/gea.20325

Dillehay, T. D. (1999). The late Pleistocene cultures of South America. *Evolutionary Anthropology: Issues, News, and Reviews*, *7*, 206–216. https://doi.org/10.1002/(SICI)1520-6505(1999)7:6%3C206::AID-EVAN5%3E3.0.CO;2-G

Dillehay, T. D. (2008). Profiles in Pleistocene history. In: H. Silverman & W. H. Isbell (Eds.), *The Handbook of South American Archaeology*, (pp. 29-43). Springer.

Dillehay, T. D., Calderón, G. A., Politis, G., & Beltrão, M. C. (1992). Earliest hunters and gatherers of South America. *Journal of World Prehistory*, *6*, 145–204. https://doi.org/10.1007/BF00975549

Dunnell, R. C., & Stein, J. K. (1989). Theoretical issues in the interpretation of microartifacts. *Geoarchaeology*, *4*, 31–41. https://doi.org/10.1002/gea.3340040103

Egli, R. (2004). Characterization of individual rock magnetic components by analysis of remanence curves: 1. Unmixing natural sediments. *Studia Geophysica et Geodaetica*, *48*, 391–446. https://doi.org/10.1023/B:SGEG.0000020839.45304.6d

Embrapa—Empresa Brasileira de Pesquisa Agropecuária. (2006). *Sistema Brasileiro de classificação de solos* (2nd ed.). Centro Nacional de Pesquisa de Solos.

Evans, M. E., & Heller, F. (2003). *Environmental magnetism: Principles and applications of enviromagnetics*. Academic Press.

Fagan, B. (1987). *The great journey. The peopling of ancient America*. Thames and Hudson.

FAO—Food and Agriculture Organization. (2014). *World Reference Base for Soil Resources 2014: International Soil Classification System for Naming Soils and Creating Legends for Soil Maps*. FAO, Rome, Italy (World Soil Resources Reports, 106).

Fiedel, S. J. (2017). Did monkeys make the pre-Clovis pebble tools of Northeastern Brazil? *PaleoAmerica*, *3*, 6–12. https://doi.org/10.1080/20555563.2016.1273000

Fúlfaro, V. J., & Suguio, K. (1968). A formação Rio Claro (Neocenozóico) e seu ambiente de deposição. *Revista do Instituto Geográfico e Geológico*, *20*, 45–60.

Galbraith, R. F., & Roberts, R. G. (2012). Statistical aspects of equivalent dose and error calculation and display in OSL dating: An overview and some recommendations. *Quaternary Geochronology*, *11*, 1–27.

Gouveia, S. E. M., Pessenda, L. C. R., Aravena, R., Boulet, R., Scheel-Ybert, R., Bendassoli, J. A., Ribeiro, A. S., & Freitas, H. A. (2002). Carbon isotopes in charcoal and soils in studies of paleovegetation and climate changes in the late Pleistocene and the Holocene in the southeast and centerwest regions of Brazil. *Global and Planetary Change*, *33*, 95–106. https://doi.org/10.1016/S0921-8181(02)00064-4

Gruhn, R. (1977). Earliest man in the Northeast: A hemisphere-wide perspective. *Annals of the New York Academy of Sciences*, *288*, 163–164. https://doi.org/10.1111/j.1749-6632.1977.tb33609.x

Gruhn, R. (1988). Linguistic evidence in support of the coastal route of earliest entry into the New World. *Man*, *23*, 77–100. https://doi.org/10.2307/2803034

Gruhn, R., & Bryan, A. L. (1991). A review of Lynch's descriptions of South American Pleistocene sites. *American Antiquity*, *56*, 342–348. https://doi.org/10.2307/281423

Guérin, G., Mercier, N., & Adamiec, G. (2011). Dose-rate conversation factors: Update. *Ancient TL*, *29*, 5–8.

Humphreys, G. (1993). Bioturbation, biofabrics and the biomantle: An example from the Sydney Basin. *Developments in Soil Science*, *22*, 421–436. https://doi.org/10.1016/S0166-2481(08)70431-8

Hurt, W. R. (1986). The cultural relationships of the Alice Boer site, State of Sao Paulo, Brazil. In: A. L. Bryan (Ed.), *New evidence for the Pleistocene peopling of the Americas* (pp. 215–219). Center for the Study of Early Man.

Jull, A. J. T., Burr, G. S., McHargue, L. R., Lange, T. E., Lifton, N. A., Beck, J. W., Donahue, D. J., & Lal, D. (2004). New frontiers in dating geological, paleoclimatic, and anthropological applications using accdelerator mass spectometry measurements of 14C and 10Be in diverse samples. *Global and Planetary Change*, *41*, 309-323. https://doi.org/10.1016/j.gloplacha.2004.01.014.

Kooistra, M. J., & Pulleman, M. M. (2010). Features related to faunal activity, *Interpretation of micromorphological features of soils and regoliths* (pp. 397–418). Elsevier. https://doi.org/10.1016/B978-0-444-53156-8.00018-0

Kruiver, P. P., Dekkers, M. J., & Heslop, D. (2001). Quantification of magnetic coercivity components by the analysis of acquisition curves of isothermal remanent magnetization. *Earth Planetary Science Letters*, *189*, 269–276. https://doi.org/10.1016/S0012-821X(01)00367-3

Ladeira, F. S. B. (2002). *Paleossolos silicificados na Serra de Itaqueri, Itirapina/SP: Subsídios para a reconstituição paleoambiental* (PhD Dissertation). Universidade de São Paulo, São Paulo, Brazil.

Ladeira, F. S. B., & Santos, M. (2006). Tectonics and Cenozoic paleosols in Itaqueri's Hill (São Paulo-Brazil): Implications for the long-term geomorphological evolution. *Zeitschrift fur Geomorphologie, Supplementband*, *145*, 37–62.

Laming-Emperaire, A. (1975). Problèmes de préhistoire brésilienne. *Annales. Histoire, Sciences Sociales*, *30*, 1229–1260. https://doi.org/10.3406/ahess.1975.293672

Laming-Emperaire, A. (1976). Le plus ancien peuplement de l'Amérique. *Bulletin de la Société préhistorique française. Comptes rendus des séances mensuelles*, *73*, 280–287.

Liu, Q., Roberts, A. P., Larrasoaña, J. C., Banerjee, S. K., Guyodo, Y., Tauxe, L., & Oldfield, F. (2012). Environmental magnetism: Principles and applications. *Reviews of Geophysics*, *50*, RG4002. https://doi.org/10.1029/2012RG000393

Lynch, T. F. (1990). Glacial-age man in South America? A critical review. *American Antiquity*, *55*, 12–36. https://doi.org/10.2307/281490

Lynch, T. F. (1991). Lack of evidence for glacial-age settlement of South America: Reply to Dillehay and Collins and to Gruhn and Bryan. *American Antiquity*, *56*, 348–355. https://doi.org/10.2307/281424

Lynch, T. F. (1998). The Paleoindian and Archaic stages in South America: Zones of continuity and segregation. In M. Plew (Ed.), *Explorations in American archaeology: Essays in honor of Wesley Hurt* (pp. 89–100). University Press of America.

MacNeish, R. S. (1976). Early man in the New World: A survey of the archaeological evidence suggests that a number of specialized tool complexes were widely distributed in the Americas before 12,000 years ago. *American Scientist*, *64*, 316–327.

MacNeish, R. S. (1978). The Harvey Lecture Series. Late Pleistocene adaptations: A new look at early peopling of the new world as of 1976. *Journal of Anthropological Research*, *34*, 475–496. https://doi.org/10.1086/jar.34.4.3629646

Macphail, R. I., & Goldberg, P. (2010). Archaeological materials. In G. Stoops, V. Marcelino, & F. Mees (Eds.), *Interpretation of Micromorphological Features of Soil and Regoliths* (pp. 589–622). Elsevier.

Maxbauer, D. P., Feinberg, J. M., & Fox, D. L. (2016a). Magnetic mineral assemblages in soils and paleosols as the basis for paleoprecipitation proxies: A review of magnetic methods and challenges. *Earth-Science Reviews*, *155*, 28–48. https://doi.org/10.1016/j.earscirev.2016.01.014

Maxbauer, D. P., Feinberg, J. M., & Fox, D. L. (2016b). MAX UnMix: A web application for unmixing magnetic coercivity distributions. *Computers and Geosciences*, *95*, 140–145. https://doi.org/10.1016/j.cageo.2016.07.009

Meis, M. R. M., & Beltrão, M. C. (1981). The Alice Boer site: Lithostratigraphic background, *Union Internacional de Ciencias Prehistoricas y Protohistoricas, XX Congresso* (pp. 99–100). Comision XII.

Meis, M. R. M., & Beltrão, M. C. (1982). Nota prévia sobre a sedimentação neoquaternária em Alice Boer – Rio Claro, SP. *Atas do IV Simpósio do Quaternário no Brasil*, (pp. 401-414). Rio de Janeiro.

Melo, M. S. (1995). *A Formação Rio Claro e depósitos associados: Sedimentação neocenozóica na Depressão Periférica Paulista* (Unpublished PhD Dissertation). Universidade de São Paulo, São Paulo, Brazil.

Milani, E. J., & Zalan, P. V. (1999). An outline of the geology and petroleum systems of the Paleozoic interior basins of South America. *Episodes-Newsmagazine of the International Union of Geological Sciences*, *22*, 199–205.

Moreno de Sousa, J. C. (2019). *Tecnologia de Ponta a Ponta: Em Busca de Mudanças Culturais Durante o Holoceno em Indústrias Líticas do Sudeste e Sul do Brasil* (PhD Dissertation). Federal University of Rio de Janeiro, Rio de Janeiro, Brazil.

Murray, A. S., & Wintle, A. G. (2000). Luminescence dating of quartz using an improved single-aliquot regenerative-dose protocol. *Radiation Measurements*, *32*, 57–73. https://doi.org/10.1016/S1350-4487(99)00253-X

O'Brien, M. J., Boulanger, M. T., Collard, M., Buchanan, B., Tarle, L., Straus, L. G., & Eren, M. I. (2014). On thin ice: Problems with Stanford and Bradley's proposed Solutrean colonisation of North America. *Antiquity*, *88*, 606–613. https://doi.org/10.1017/S0003598X0010122X

Okumura, M., & Araujo, A. G. (2016). The Southern Divide: Testing morphological differences among bifacial points from southern and southeastern Brazil using geometric morphometrics. *Journal of Lithic Studies*, *3*(1), 107–131.

Parenti, F., Cannell, A., Debard, E., Faure, M., & Okumura, M. (2018). Genesis and taphonomy of the archaeological layers of Pedra Furada rock-shelter, Brazil. *Quaternaire. Revue de l'Association française pour l'étude du Quaternaire*, *29*, 255–269. https://doi.org/10.4000/quaternaire.10313

Penteado, M. M. (1968). *Geomorfologia do Setor Centro-Ocidental da Depressão Periférica Paulista* (PhD Dissertation), Universidade Estadual Paulista, Faculdade de Filosofia, Ciências e Letras de Rio Claro.

Pereira, E., Carneiro, C. D. R., Bergamaschi, S., & Almeida, F. F. M. (2012). Evolução das Sinéclises Paleozoicas: Províncias Solimões, Amazonas, Parnaíba e Paraná. In Y. Hasui, C. D. R. Carneiro, & F. F. M. Almeira e A. Bartorelli (Eds.), *Geologia do Brasil* (pp. 374–394). Beca.

Perez, R. A. R. (1991). *A ocupação dos Terraços Fluviais do Baixo Passa Cinco: Arqueologia Experimental* (MA Thesis). University of São Paulo, São Paulo Brazil.

Pessenda, L. C. R., Gouveia, S. E. M., & Aravena, R. (2001). Radiocarbon dating of total soil organic matter and humin fraction and its comparison with 14 C ages of fossil charcoal. *Radiocarbon*, *43*(2B), 595–601. https://doi.org/10.1017/S0033822200041242

Pessenda, L. C. R., Gouveia, S. E. M., Aravena, R., Boulet, R., & Valencia, E. P. E. (2004). Holocene fire and vegetation changes in southeastern Brazil as deduced from fossil charcoal and soil carbon isotopes. *Quaternary International*, *114*, 35–43. https://doi.org/10.1016/S1040-6182(03)00040-5

Pinheiro, M. R., & Queiroz Neto, J. P. (2014). Reflexões sobre a gênese da Serra Geral e da Depressão Periférica Paulista: O exemplo da região da Serra de São Pedro e do Baixo Piracicaba, SP. *Revista do Instituto Geológico*, *35*(1), 47–59. https://doi.org/10.5935/0100-929X.20140004

Poupeau, G., Cunha, L. M., Fonseca, M. P., Meis, M. R., Neme, S. M., Perez, R., & Souza, J. H. (1984). Une Revision Geologique-Geochronologique du Site Archeologique Alice Boer (Rio Claro, Sp $$ Bresil). Rapport d'une mission de terrain du, 9 au 13 janvier 1984. Report presented to the Centro Brasileiro de Pesquisas Físicas, Ms. No. CBPF-MO-001/84 (pp. 49).

Poupeau, G., Souza, J. H., & Rivera, A. (1984). *Thermoluminescence dating of pleistocene sediments* (Report No. CBPF-NF–016/84). Unpublished report, Centro Brasileiro de Pesquisas Fisicas.

Prescott, J. R., & Hutton, J. T. (1988). Cosmic ray and gamma ray dose dosimetry for TL and ESR. *Nuclear Tracks and Radiation Measurements*, *14*, 223–235. https://doi.org/10.1016/1359-0189(88)90069-6

Prous, A. (1995). Archaeological analysis of the oldest settlements in the Americas. *Revista Brasileira de Genética*, *18*, 689–699.

Prous, A., & Fogaça, E. (1999). Archaeology of the Pleistocene-Holocene boundary in Brazil. *Quaternary International*, *53*, 21–41. https://doi.org/10.1016/S1040-6182(98)00005-6

Reimerr, P. J., Baillie, M. G. L., Bard, E., Bayliss, A., Beck, J. W., Blackwell, P. G., Bronk Ramsey, C., Buck, C. E., Burr, G. S., Edwards, R. L., Friedrich, M., Grootes, P. M., Guilderson, T. P., Hajdas, I., Heaton, T. J., Hogg, A. G., Hughen, K. A., Kaiser, K. F., Kromer, B., … Weyhenmeyer, C. E. (2009). IntCal09 and Marine09 radiocarbon age calibration curves, 0–50,000 years cal BP. *Radiocarbon*, *51*(4), 1111–1150.

Ricci, O. (2018). *Microartefatos e Análise Geoarqueológica: Um Estudo de Caso da Região de Rio Claro—SP* (MA Thesis). Museum of Archaeology and Ethnology, University of São Paulo, São Paulo, Brazil.

Riris, P., Oliver, J. R., & Mendieta, N. L. (2018). Missing the point: Re-evaluating the earliest lithic technology in the Middle Orinoco. *Royal Society Open Science*, *5*, 180690. https://doi.org/10.1098/rsos.180690

Roosevelt, A. C. (1998). Ancient and modern hunter-gatherers of lowland South America: An evolutionary problem. In: Balée, W. (Ed.) *Advances in historical ecology* (pp. 190-212). Columbia University Press.

Ross, J. L. S., & Moroz, I. C. (1997). Mapa Geomorfológico do Estado de São Paulo. *Revista do Departamento de Geografia*, *10*, 41–58. https://doi.org/10.7154/RDG.1996.0010.0004

Santos, R. D., Lemos, R. C., Santos, H. G., Ker, J. C., & Anjos, L. H. C. (2005). *Manual de Descrição e Coleta de Solo no Campo* (5th ed.). SBCS.

Scheinsohn, V. (2003). Hunter-gatherer archaeology in South America. *Annual Review of Anthropology*, *32*(1), 339–361. https://doi.org/10.1146/annurev.anthro.32.061002.093228

Schmitz, P. I. (1990). O povoamento pleistocênico do Brasil. *Revista de Arqueología Americana*, *1*, 33–68.

Stanford, D. J., & Bradley, B. A. (2012). *Across Atlantic Ice: The Origin of America's Clovis Culture*. University of California Press.

Steeves, P. F. (2015). Decolonizing the Past and Present of the Western Hemisphere (The Americas). *Archaeologies: Journal of the World Archaeological Congress*, *11*, 42–69. https://doi.org/10.1007/s11759-015-9270-2

Stoops, G., Marcelino, V. & Mees, F., (Eds.). (2018). *Interpretation of micromorphological features of soils and regoliths*. Elsevier.

Troncoso, L. P. S., Corrêa, A., & Zanettini, P. (2016). Paleoíndios em São Paulo: Nota a respeito do sítio Caetetuba, Município de São Manuel, SP. *Palaeoindian Archaeology*, *1*, 50–71.

Udden, J. A. (1914). Mechanical composition of some clastic sediments. *Geological Society of America Bulletin*, *25*, 655–744. https://doi.org/10.1130/GSAB-25-655

Vance, E. (1989). *The role of microartifacts in spatial analysis* (PhD Dissertation). University of Washington, Seattle, WA.

Vialou, D., Benabdelhadi, M., Feathers, J., Fontugne, M., & Vialou, A. V. (2017). Peopling South America's centre: The late Pleistocene site of Santa Elina. *Antiquity*, *91*(358), 865–884.

Watling, J., Iriarte, J., Mayle, F. E., Schaan, D., Pessenda, L. C., Loader, N. J., Street-Perrott, F., Dickau, R., Damasceno, A., & Ranzi, A. (2017). Impact of pre-Columbian "geoglyph" builders on Amazonian forests. *Proceedings of the National Academy of Sciences*, *114*, 1868–1873. https://doi.org/10.1073/pnas.1614359114

Weninger, B., Jöris, O., & Danzeglocke, U. (2012). *Calpal-2007. Cologne Radiocarbon Calibration, Palaeoclimate Research Package*. http://www.calpal.de/

Wentworth, C. K. (1922). A scale of grade and class terms for clastic sediments. *Journal of Geology*, *30*, 377–392. https://doi.org/10.1086/521238

Whitley, D. S., & Dorn, R. I. (1993). New perspectives on the Clovis vs. pre-Clovis controversy. *American Antiquity*, *58*, 626–647. https://doi.org/10.2307/282199

Wintle, A. G., & Murray, A. S. (2006). A review of quartz optically stimulated luminescence characteristics and their relevance in single-aliquot regeneration dating protocols. *Radiation Measurements*, *41*, 369–391. https://doi.org/10.1016/j.radmeas.2005.11.001

Zaine, J. E. (1994). *Geologia da Formação Rio Claro na folha Rio Claro (SP)* (MA Thesis). Universidade Estadual Paulista, Rio Claro, Brazil.

How to cite this article: de Mello Araujo AG, Feathers JK, Hartmann GA, et al. Revisiting Alice Boer: Site formation processes and dating issues of a supposedly pre-Clovis site in Southeastern Brazil. *Geoarchaeology*. 2020;1–27. https://doi.org/10.1002/gea.21831